Regulation of Cav2.1 by Ankyrin B and its variants

by

Catherine S.W. Choi
Hons. B.Sc. – University of British Columbia – 2008
Juris Doctor – University of British Columbia – 2013

A Thesis Submitted in Partial Fulfillment
of the Requirements for the Degree of

MASTER OF SCIENCE

in the Division of Medical Sciences

Supervisory Committee

Regulation of Cav2.1 by Ankyrin B and its variants

by

Catherine S.W. Choi
Hons. B.Sc. – University of British Columbia – 2008
Juris Doctor – University of British Columbia – 2013

Supervisory Committee

Dr. Leigh Anne Swayne, Division of Medical Sciences
Supervisor

Dr. Laura Arbour, Division of Medical Sciences
Departmental member

Dr. Raad Nashmi, Department of Biology
Outside member

Abstract

Ankyrin B (AnkB) is a scaffolding protein, acting as a bridge between ion channels and cytoskeleton networks. AnkB variants are associated with cognitive disorders including autism spectrum disorder and epilepsy. In the brain, AnkB interacts with Cav2.1, the pore-forming subunit of P/Q type voltage gated calcium channels. However, how AnkB regulates Cav2.1 is not fully understood. Using HEK293T cells, we discovered that AnkB increases Cav2.1 expression levels but does not change Cav2.1 surface levels. AnkB p.S646F increases Cav2.1 to an even greater level of expression, again without impacting Cav2.1 surface levels. Looking at a partial loss of AnkB in glutamatergic neurons, overall Cav2.1 levels decreased at P30 but the synaptosomal fraction was not impacted. Our findings indicate that AnkB plays a role in regulating an intracellular pool of Cav2.1 but does not affect the surface or the synaptosomal pools of Cav2.1. This intracellular pool of Cav2.1 may play an important role in neuronal function and homeostasis, suggesting a mechanism for neuronal pathogenicity of AnkB variants.

Table of Contents

List of Tables

List of Figures

List of Abbreviations

AIS: Axon initial segment

AnkB: Ankyrin B

$AnkB^{glut+/-}$: AnkB conditional heterozygous knockout, $AnkB^{flox/wt}$: $Emx1^{IRES-cre}$

ASD: Autism spectrum disorder

ER: Endoplasmic reticulum

GAPDH: Glyceraldehyde 3-phosphate dehydrogenase

GLUT4: Glucose transporter 4

IP3R: Inositol-trisphosphate receptor

L1CAM: L1 cell adhesion molecule

NCX1: Na^+/Ca^{2+} exchanger type 1

NKA: Na^+/K^+ ATPase

PI3P: Phosphatidylinositol 3-phosphate

PKC: Protein kinase C

PM: Plasma membrane

PSD95: Postsynaptic density protein 95

RIM: Rab3 interacting molecules

SNARE: soluble N-ethylmaleimide-sensitive fusion protein attachment protein receptors

TfR: Transferrin Receptor

VGCC: Voltage gated calcium channels

Acknowledgments

This thesis would not have come to fruition without the support and encouragement of so many people. First and foremost, I would like to thank Dr. Leigh Anne Swayne. Without her guidance and mentorship, I would not have been able to climb this next step in my scientific career. She not only challenged me to push past familiar territories, but also supported my growth and ambitions. Also, I like to thank Dr. Laura Arbour, who always found time to help me with my project and complete tedious applications. To my committee, Drs. Swayne, Arbour, and Raad Nashmi, thank you for your invaluable advice and expertise that helped shaped this project.

Of course, a big thank you to my fellow labmates who make the lab a joy work in. Thank you to Dr. Juan Sanchez-Arias for his mice expertise and our hallway brainstorming chats. His enthusiasm for science was priceless on long experimental days. Thank you to Sarah Ebert, who wears many hats and excels at them all. Thank you to Anna Epp. Her kindness and friendship has been a highlight on this journey. Her support and our many coffee walks have made this thesis possible

Thank you to my family (Chois, Sundqvist, and Glassfords!), for your support and understanding when I decided to work over weekends. Most importantly, thank you to my partner, Jesse Glassford. He has been an unwavering support. His belief in me has sustained me through trying times and has been an essential component to completing this thesis.

This research could not have been possible without various funding support. I was supported by the University of Victoria Fellowship Graduate Awards. Also, I wish to acknowledge the contributions of the Gitxsan, who participated as partners in research to

identify the ANK2 p.S646F variant. The CIHR Bridge Funding that helped fund my research is a result of that partnership. Additionally, electrophysiology experiments would not have been possible without collaboration with Dr. Gerald W. Zamponi who was supported by the Natural Sciences and Engineering Research Council.

1. Introduction

1.1 Thesis overview

Ankyrin B (AnkB) is a scaffolding protein expressed in the heart, pancreas, and brain, where it interacts with various ion channels and the spectrin cytoskeleton network (Scotland et al. 1998; Smith & Penzes 2018; Bennett & Healy 2009; Koenig & Mohler 2017; Lorenzo et al. 2015). AnkB variants in human populations have been associated with cardiac abnormalities, with symptoms varying from sudden death to cardiac arrhythmia, as well as neurological disorders including autism spectrum disorder (ASD) and epilepsy (Koenig & Mohler 2017; Iossifov et al. 2014; Rubeis et al. 2014; Guo et al. 2017). A recently discovered variant, AnkB p.S646F, is associated with seizures, leading us to investigate AnkB's role in neuronal function (Swayne et al. 2017). AnkB interacts with an important neuronal voltage gated calcium channel, Cav2.1, whose loss-of-function mutations also lead to epilepsy and cognitive defects (Kline et al. 2014; Damaj et al. 2015). This led us to speculate that regulation of Cav2.1 by AnkB may be the underlying mechanism behind pathogenicity of AnkB variants.

In my thesis, I used biochemical and electrophysiological techniques to explore the effects of wildtype and variant AnkB on Cav2.1 expression, activity, and localization. **I hypothesized that AnkB and AnkB variants impact Cav2.1 expression levels and/or localization.** I discovered that wildtype AnkB and AnkB p.S646F led to higher Cav2.1 expression levels, but did not alter Cav2.1 cell surface expression levels, suggesting regulation of an intracellular pool of Cav2.1. In addition, I investigated the effect of partial loss of AnkB in mouse cortex, and discovered that partial loss of AnkB led to a decrease in Cav2.1 whole cortex lysate with no effect on Cav2.1 synaptosomal

fraction. This work provides insight into the relationship between AnkB and Cav2.1 and a potential mechanism of AnkB pathogenicity through Cav2.1 regulation.

This is a manuscript-based thesis. As such, Chapter 1 contains an overview of ankyrins and voltage gated calcium channels (VGCC). I will provide a general introduction to the structure and roles of ankyrins and VGCC with a focus on AnkB and Cav2.1 respectively. Chapter 2 contains the manuscript submitted for publication. Lastly, Chapter 3 expands on the discussion provided in the manuscript and will delve into the implication of this work and potential future directions.

1.2 Introduction to ankyrins

Ankyrin R (AnkR) was first discovered in erythrocytes as a spectrin interactor (Bennett 1979). Since then, the ankyrin family has expanded to include AnkB and AnkG. As the first ankyrin discovered, AnkR provided the first evidence of ankyrin's role as a scaffold, by serving as a bridge between the anion exchanger to spectrin (Bennett & Stenbuck 1980). This spectrin network makes up a part of a cell's cytoskeleton, is composed of alpha and beta spectrins, and associates with actin filaments as well as the membrane bilayer (Bennett & Lorenzo 2013). Therefore, ankyrin plays an important role in linking ion channels to the actin-spectrin backbone, anchoring ion channels to specific subcellular locations. The three ankyrins are widely expressed with AnkB and AnkG expressed in the heart, brain, skeletal muscle, lung, and kidney, and AnkR expressed in the heart, brain, skeletal muscle, and erythrocyte (Cunha & Mohler 2009). All three ankyrins have a similar structure that allows it to serve as a scaffold.

1.2.1 Ankyrin structure

Ankyrins are composed of a membrane binding domain, spectrin binding domain, and a C-regulatory domain. The membrane domain has 24 ankyrin repeats, which are 33-residue motifs found in numerous unrelated proteins (Michaely et al. 2002). Ankyrin repeats are formed from anti-parallel alpha helices connected by beta-hairpins that extends outwards almost at a 90 degree which forms an “ankyrin groove” (Islam et al. 2018) (Fig 1.1). The “ankyrin groove” is considered to be the main interacting surface. The repeat structure lends itself well to interacting with multiple proteins, with numerous interaction sites. Specifically, the membrane binding domain of ankyrins is the interaction site for a variety of ion channels (Yamankurt et al. 2012). The spectrin binding domain is comprised of two ZU5 and a UPA domain and binds to spectrins (Bennett & Healy 2009). The C-regulatory domain is comprised of a death domain and a largely unstructured region. Although it contains the conserved death domain, there is no known association with typical functions such as interactions with other death domains or apoptosis pathways. The C-terminal unstructured region is believed to regulate AnkB itself through intramolecular interactions and can regulate AnkB subcellular localization in cardiomyocytes (Wang et al. 2014; Abdi et al. 2006; Mohler et al. 2002). AnkB and AnkG have a giant splice variant (440 and 480 kDa respectively), arising from an additional 220 kDa of random coil between the spectrin binding domain and death domain.

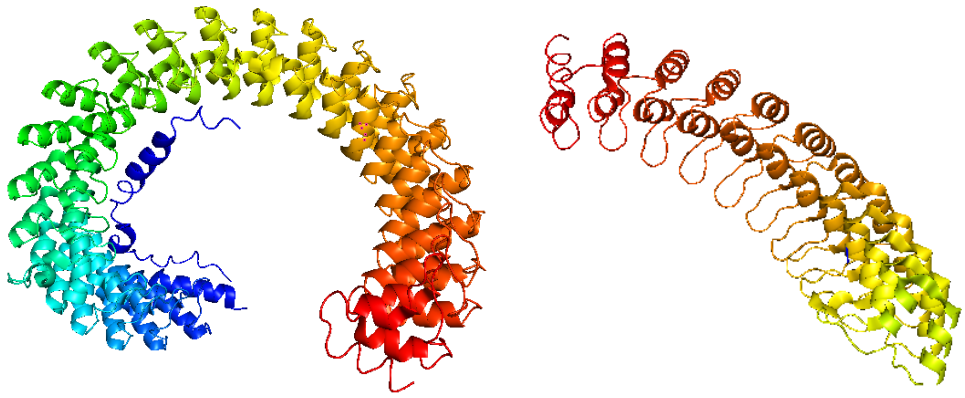

Figure 1.1 Structure of AnkB MBD complexed with AnkR autoinhibition region. View of 24 ankyrin repeats (AnkB membrane binding domain) and autoinhibition region (AnkR C-regulatory domain) (left) and alternate view of the first 12 ankyrin repeats (right). Ankyrin repeats are shown here as alpha helices with beta loops extended outwards shown in spectrum from red to blue. The AnkR autoinhibition region is shown in dark blue complexed with the membrane binding domain. (Generated using PyMOL, PDB 4rlv) (Wang et al. 2014)

1.2.2 Scaffold to ion channels

The distinct structure of ankyrins allows them to bind to multiple partners and serve as a bridge between different proteins. AnkB acts as scaffolding protein, anchoring a variety of ion channels to a specific subcellular location. For example, AnkB interacts with Na^+/K^+ ATPase (NKA), Na^+/Ca^{2+} exchanger 1 (NCX1), and inositol 1,4,5-triphosphate receptors (IP3R), and anchors them to microdomains at T-tubules of cardiomyocytes (Mohler et al. 2005). The co-localization of these channels is believed to be due, in part, to AnkB, as partial loss of AnkB leads to decrease expression and localization of these ion channels at T-tubules (Mohler et al. 2005; Cunha et al. 2007). Of

particular interest is the inability of AnkB variants to rescue channel localization, pointing to a key role for AnkB in securing these ion channels to their proper place. AnkB p.E1425G (referred to as p.E1458G in the construct used here) mutation interferes with AnkB binding to NKA, NCX1, and IP3R, and cannot rescue mislocalization of these channels in $AnkB^{+/-}$ cardiomycytes (Mohler et al. 2005; Mohler et al. 2004). AnkB p.S646F is also unable to rescue NCX1 mislocalization (Swayne et al. 2017). The mislocalization of NKA, NCX1, and IP3R by loss of AnkB led to abnormalities in cardiomyocytes, including reduced spontaneous contraction and abnormal patterns of cytoplasmic calcium release (Peter J. Mohler, Le Scouarnec, Denjoy, Lowe, Guicheney, Caron, Driskell, J.-J. Schott, et al. 2007).

Similarly, in the brain, AnkB serves as a scaffold for multiple channels composed of NCX1, IP3R, and calcium pump type 2 (Lencesova et al. 2004). These channels co-localize to plasma membrane-endoplasmic reticulum (PM-ER) microdomains, allowing these channels to work in concert with each other. AnkB also interacts with Cav2.1, 2.2 and Cav3, the pore forming subunit of P/Q, N, and T type voltage gated calcium channels (VGCC) respectively (Kline et al. 2014; Garcia-Caballero et al. 2018). Decreasing AnkB expression in neurons significantly decreased expression of Cav2.1, 2.2 and Cav3.2, potentially affecting neuronal function. AnkB is also known to interact with L1 cell adhesion molecule (L1CAM) in cerebellar neurons. AnkB-L1CAM interaction promotes L1CAM stationary behaviour and is involved in L1CAM diffusion movements on the cell surface (Gil et al. 2003).

In addition to its role in cardiomyocytes and neurons, AnkB also regulates ion channels in other systems. In adipocytes, AnkB regulates the cell surface expression of

glucose transporter 4 (GLUT4) (Lorenzo et al. 2015). AnkB variants led to increase surface expression of GLUT4 by reducing internalization rate. As such, AnkB plays an important role in the regulation of multiple ion channels in multiple systems.

1.2.3 Adaptor to motor proteins

In addition to anchoring channels to subcellular membranes, AnkB can also act as a bridge between specific cargo and motor proteins (Lorenzo et al. 2014). Long range transportation is particularly important in neurons with long axons, requiring efficient transportation of proteins to and from the cell periphery. AnkB plays a part in this long range transportation by interacting with phosphatidylinositol 3-phosphate (PI(3)P), a lipid enriched in membranes of the endolysosomal autophagosomal pathway, and p62, a subunit of the dynactin motor complex (Lorenzo et al. 2014; Devereaux et al. 2013; Liu 2017). The PI(3)P- and p62- interaction with AnkB occurs via AnkB spectrin binding domain (Lorenzo et al. 2014). In AnkB knockout neurons, vesicles containing synaptophysin (synaptic), Rab5 (endosomes), and LAMP1 (lysosomes) all had slower velocities in axons, whereas the velocities of dendritic vesicles containing transferrin receptor were unchanged. As well, AnkB recruits RabGAP1L to PI(3)P positive vesicles, inactivating Rab22A and playing a role in endosome maturation (Qu et al. 2016). By acting as a bridge between different proteins, AnkB plays a role in subcellular trafficking ensuring proper localization, trafficking, and neuronal function.

1.2.4 Subcellular distribution

Since AnkB influences the subcellular localization of its interactors, the subcellular localization of AnkB itself can shed light on its function in neurons. In cultured hippocampal neurons, endogenous AnkB is found in the cell body, dendrites,

axon, and growth cone, but is excluded from the axon initial segment (AIS) (Lorenzo et al. 2014; Galiano et al. 2012). *In vivo,* AnkG is localized at the nodes of Ranvier, the gaps between myelination by oligodendrocytes or Schwann cells of the central or peripheral nervous system respectively (Ogawa 2006; Ho et al. 2014; Chang et al. 2014). AnkB is localized close by at paranodal junctions, the regions flanking nodes of Ranvier. Notably, AnkG is present at the axon initial segment and nodes of Ranvier, where AnkB is excluded. Additionally, increasing and decreasing AnkB expression impacts the length of the AIS and AnkG localization, suggesting a coordination between AnkB and AnkG (Galiano et al. 2012). At the synapse, the connection between neurons, AnkB was found in multiple mass spectrometry identifications of purified postsynaptic density samples (Collins et al. 2006; Jordan et al. 2004; Peng et al. 2004). Looking specifically at intracellular localization in mouse embryonic fibroblast, AnkB co-localized mainly with early and recycling endosome and lysosomes, with almost no co-localization with golgi or ER membranes (Qu et al. 2016).

1.2.5 Associated Diseases

AnkB knockout mice are born in Mendelian ratios suggesting normal embryonic development, but 95% are dead or dying by postnatal day 8 (Scotland et al. 1998). In humans, mutations in AnkB can lead to diseases. AnkB variants have been associated with various disorders, most notably Ankyrin B syndrome. Ankyrin B syndrome comprises of bradycardia, sinus arrhythmia, delayed conduction, type 4 long QT syndrome, and increase risk of sudden death (Peter J. Mohler, Le Scouarnec, Denjoy, Lowe, Guicheney, Caron, Driskell, J. J. Schott, et al. 2007; Peter J Mohler et al. 2007). The recent discovery of AnkB variant p.S646F by our group has broadened the AnkB

syndrome phenotype to also include Wolff-Parkinson-White syndrome/tachycardia, congenital heart malformation, and cardiomyopathy with associated sudden death (Swayne et al. 2017). In addition to heart abnormalities, AnkB has also been implicated in obesity and type 2 diabetes. AnkB variant p.R1788W is enriched in the population with type 2 diabetes (Lorenzo et al. 2015; Lorenzo & Bennett 2017). AnkB p.R1778W variant knock in mice exhibit primary pancreatic beta cell insufficiency and age-dependent adiposity (Lorenzo et al. 2015). AnkB is also associated with neurological disorders. Using whole exome analysis of individuals with ASD, AnkB was identified as a strong ASD gene candidate (Iossifov et al. 2014; Rubeis et al. 2014). In addition, using protein-protein interaction network analysis with a random walk restart algorithm, AnkB was identified as a core candidate gene for epilepsy (Guo et al. 2017). Research from our own group discovered that some carriers of AnkB p.S646F exhibited symptoms consistent with seizure (Swayne et al. 2017).

1.3 Introduction to voltage gated calcium channels

As mentioned above, AnkB interacts with voltage gated calcium channels (VGCC). VGCC are composed of a main pore-forming subunit ($Cav\alpha_1$) and accessory subunits ($Cav\alpha_2\delta$, $Cav\beta$, and $Cav\gamma$) (Catterall 2011; Weiss & Zamponi 2017). Early studies into calcium channels categorized VGCC based on their electrophysiological properties and response to different inhibitors, naming them L-, P/Q-, N-, R-, or T- type (Tsien & Barrett n.d.). With advances in technologies, these different types of VGCC are now categorized by the pore-forming $Cav\alpha_1$ subunit, encoded by 10 genes that can be separated into Cav1, 2, or 3, based on their sequence similarities. VGCC can be characterized as high-voltage activated channels, including Cav1 (L-type) and Cav2

(P/Q-, N-, and R- type), and low-voltage activated channels, Cav3 (T-type) (Table 1.1). VGCCs play an important role in cellular function by providing a gated entryway for calcium, an important second messenger. Calcium can trigger various pathways and responses from contraction and secretion to protein phosphorylation and gene transcription (Catterall 2011).

Table 1.1 List of VGCC

Voltage activated	**Current**	**Cavα_1**	**Gene**
High	L-type	Cav1.1	*CACNA1S*
		Cav1.2	*CACNA1C*
		Cav1.3	*CACNA1D*
		Cav1.4	*CACNA1F*
	P/Q-type	Cav2.1	*CACNA1A*
	N-type	Cav2.2	*CACNA1B*
	R-type	Cav2.2	*CACNA1E*
Low	T-type	Cav3.1	*CACNA1G*
		Cav3.2	*CACNA1H*
		Cav3.3	*CACNA1I*

1.3.1 Structure of Cavα_1 and accessory subunits

All Cavα_1 have a similar structure, composed of four homologous domains (I-IV), each with 6 transmembrane segments (S1-6) (Fig.1.2) (Simms & Zamponi 2014). Between each domain are cytoplasmic linkers and the 4 domains are flanked by cytoplasmic N- and C- terminal tails. Within the S4 segments lie the residues that control voltage-dependent activation, while the region between S5 and S6 forms the highly selective pore. Four genes encode for Cavβ_{1-4} (Buraei & Yang 2010). Cavβ subunit binds to the alpha interaction domain (AID) region in the Cavα_1 I-II linker and alters Cav function. There are also 4 different Cav$\alpha_2\delta_{1-4}$ subunits (Dolphin 2018). Cav$\alpha_2\delta$ is a single protein that is post-translationally cleaved, but remains held together by a disulfide bond.

Cav$\alpha_2\delta$ is situated on the extracellular surface. The δ portion has a short hydrophobic stretch with a potential transmembrane domain and a glycosylphosphatidylinositol modification that anchors Cav$\alpha_2\delta$ to the plasma membrane (Davies et al. 2010). Cav$\alpha_2\delta$ is heavily glycosylated (Jay et al. 1991). Lastly, the Cavγ subunit was originally found in skeletal muscle, and later new homologues were found in other tissues (Weiss & Zamponi 2017). It has been shown to affect Cavα_1 as well as AMPA and kainate receptors. With all the Cav subunits, multiple alternative splicing exists for each gene.

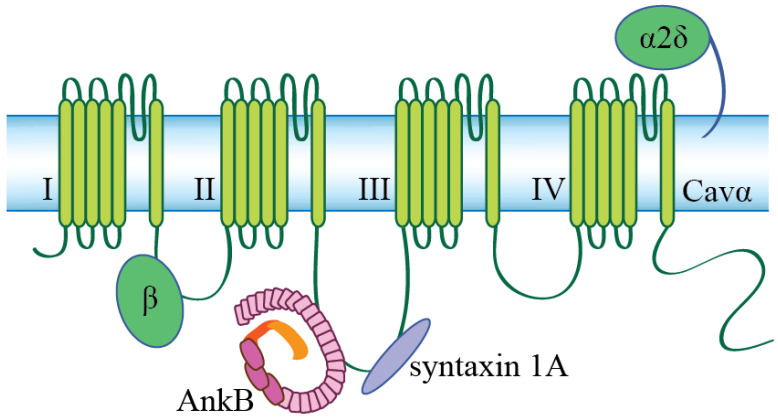

Figure 1.2 Structure of VGCC

Cavα_1 has 4 homologous domains connected by intracellular linkers. Cav$\alpha_2\delta$ is on the extracellular surface while Cavβ interacts with the intracellular I-II linker. AnkB and syntaxin 1A both interacts with the II-III linker

1.3.2 Regulation by accessory subunits

The Cavβ subunit increases Cavα_1 surface expression by regulating endoplasmic reticulum (ER) retention/export signal and preventing ubiquitination and proteasomal degradation. In addition to regulating Cavα_1 expression and localization, Cavβ also regulates channel gating, affecting activation voltage and speed. Originally, studies

looking at the localization of Cav2.1 I-II region, supported the idea that the I-II linker contained an ER retention signal that is suppressed by interactions with Cavβ (Bichet et al. 2000). Subsequent studies suggested a more complicated picture, whereby Cavβ promotes an ER export signal in the I-II linker shifting the localization signal away from retention signals elsewhere in the channel (Maltez et al. 2005; Cornet et al. 2002; Fang & Colecraft 2011). Cavβ is also believed to play a role in Cavα_1 proteostasis through ER-associated degradation pathway involving ubiquitination and proteasomal degradation. Cav1.2 expression increases in the presence of Cavβ (Altier et al. 2011). Cavβ appears to interfere with the binding of Cav1.2 to derlin and p97, proteins involved ER-associated degradation and prevents ubiquitination of Cav1.2. Similarly, the I-II loop of Cav2.2 is also ubiquitinated and degraded in the absence of Cavβ (Page et al. 2016). Ubiquitination is required for efficient degradation by the proteasome. Recently the ubiquitin ligase for Cav2.1 was discovered. This new interactor, RNF138, plays a key role in Cav2.1 protein stability (Fu et al. 2017). In the presence of RNF138, Cav2.1 expression is reduced and polyubiquitination increased. This affect is attenuated in the presence of Cavβ. As such, Cavβ subunit plays an important role in regulating the Cavα_1 trafficking and protein stability.

Like Cavβ, Cav$\alpha_2\delta$ also alters channel expression and function, generally by increasing Cavα_1 surface density and altering activation kinetics (Dolphin 2018). Cav$\alpha_2\delta$ increases calcium current density of Cav1 and Cav2. Mutations of key glycosylation sites on Cav$\alpha_2\delta$ prevent increase in peak current density of Cav1.2 (Tétreault et al. 2016). Looking at cell surface expression levels, Cav2.2 had increased surface levels in the presence of Cav$\alpha_2\delta_1$ with even greater levels when Cavβ_1 was present as well (Cassidy et

al. 2014). In addition, Cav$\alpha_2\delta$ appears to decrease the internalization of Cav2.2, suggesting one mechanism by which Cav$\alpha_2\delta$ alters calcium currents (Bernstein & Jones 2007). Gabapentin, an anticonvulsant and analgesic, binds to Cav$\alpha_2\delta$ and can reduce P- and N- type calcium currents (Patel & Dickenson 2016). As well, a study showed that gabapentin reduces Cav2.2 surface, without disrupting the Cav2.2- Cav$\alpha_2\delta_1$ interaction (Cassidy et al. 2014).

1.3.3 Role at the presynapse

At the presynapse, Cav2.1 is situated close to neurotransmitter active zones (He et al. 2018). The opening of calcium channels leads to a localized increase of calcium concentration, triggering nearby soluble N-ethylmaleimide-sensitive fusion protein (NSF) attachment protein receptor (SNARE) complex and subsequent vesicle fusion and neurotransmitter release. SNARE is a family of proteins essential for membrane fusion. At the presynapse, SNARE complex involves syntaxin 1A, SNAP25, and synaptobrevin (Mochida 2000). Synaptobrevin is present on the vesicle membrane while syntaxin 1A and SNAP25 are on the target-membrane. These three proteins form a coil-coil interaction of their alpha-helices, followed by fusion of the opposing membranes. Cav2.1 interacts with syntaxin 1A and SNAP25 through its *syn*aptic *pr*otein *int*eraction site (synprint) in the II-III loop (Rettig et al. 1996). Syntaxin 1A and SNAP25 themselves can modulate Cav2.1 activity (Wiser et al. 1996). In addition, Cav2.1 interacts with scaffolding protein Rab3 interacting molecules (RIMs) and RIM binding proteins, and these scaffolds can modulate Cav2.1 targeting to presynaptic active zones (Hirano et al. 2017; Kaeser et al. 2011). Regulation and availability of Cav2.1 activity at the presynapse contributes to synaptic plasticity (Catterall et al. 2013). Disruption of Cav2.1 regulation

by Cav2.1 mutation in mice led to impaired long term plasticity and deficits in spatial learning and memory (Nanou et al. 2016).

1.3.4 Role at the postsynapse

Cav2.1 is best known for its role at the presynapse as the VGCC involved in neurotransmitter release. However, it is also found in non-presynaptic regions. In GABAergic mouse cortical neurons, Cav2.1 was localized to both the somatodendritic compartment as well as the axon terminals (Timmermann et al. 2002). Using an isoform specific antibody, Cav2.1 BI-specific isoform was localized mainly to the axon, while the rBA specific isoform was localized to the somatodendritic compartment. In cortical neurons, Cav2.1 co-localized with both synaptophysin, a presynaptic marker, as well as postsynaptic density protein 95 (PSD95), a postsynaptic marker (Fu et al. 2017). As well, Cav2 interacts with GluA2/3 in rabbit brain (Kang et al. 2006). Electrophysiology study suggested functional coupling of GluA1 with Cav2.1 (Kang et al. 2006). This is further supported by the co-localization of Cav2.1 with GluA1 at Purkinje cell dendritic spines (Indriati et al. 2013).

1.3.5 Role in intracellular compartment

Away from the synapse, Cav2.1 may have additional roles in neuronal function. As mentioned previously, Cav2.1 localized to the somatodendritic compartment, and may have a function outside of synaptic compartments. Looking at the roles of other VGCCs can shed light on the role of intracellular Cav2.1

An intracellular pool of Cav2.2 was observed in IMR32 neuroblastoma cells and was enriched in subcellular fractions for secretory granules (Passafaro et al. 1994; Passafaro et al. 1996). Stimulation of these cells by KCl or ionomycin triggered Cav2.2

recruitment to the cell surface. In bag cell neurons of *Aplysia californica*, protein kinase C (PKC) is translocated to the membrane upon stimulation (Zhang et al. 2008). This leads to the translocation of Cav2 from the central region to the periphery of the growth cone and then to the surface.

In cerebellar neurons, Cav2.1 co-localized with lysosomal marker LAMP1, but not early endosome marker EEA1 or ER marker calreticulin (Tian et al. 2015). In cerebellar neurons from Cav2.1 mutant mice, there was defective lysosomal fusion and little co-localization between lysosomal and autophagosomal marker. Using a membrane impermeable inhibitor, ω-agatoxin TK, there was no defect in endo-lysosomal fusion, while membrane permeable inhibitor Bepridil led to defects, suggesting that intracellular and not surface Cav2.1 played a role in lysosomal fusion. Autophagosomal maturation and lysosomal fusion is an important part of neuronal homeostasis. Without normal lysosomal fusion, damaged cellular organelles and misfolded proteins accumulate leading to neural degeneration.

1.3.6 Associated diseases

Similar to AnkB, Cav2.1 knockout mice are born in Mendelian ratio. They appear healthy until day 10 when they develop progressive neurological issues, dying at 3-4 weeks (Jun et al. 1999). Cav2.1 mutations can lead to different disorders, including spinocerebellar ataxia type 6, familial hemiplegic migraine type 1, and episodic ataxia type 2 (Schorge & Rajakulendran 2012). In addition, cases of loss of function mutations also presented with absence epilepsy and cognitive impairment including learning difficulties, attention deficiency hyperactivity disorder, and ASD (Damaj et al. 2015;

Jouvenceau et al. 2001). Individuals with Cav2.1 mutations can also show symptoms of seizures (Damaj et al. 2015; Jouvenceau et al. 2001; Imbrici et al. 2004).

1.4 Summary, hypothesis and aims

While AnkB had previously been shown to interact with Cav2.1 and regulate its levels, several important knowledge gaps remained. Scaffolding proteins are known to play roles in the localization and stability of channel proteins (Verpelli et al. 2012). For example, Cav2.1 itself is regulated by scaffolding protein RIMs (Hirano et al. 2017). Previous work demonstrated that AnkB regulates Cav2.1 levels. However, it is not clear whether AnkB regulates cell surface or intracellular Cav2.1 levels, and relatedly, whether AnkB regulates Cav2.1 localization to the cell surface. Also, mutations often alter protein function. As described above, AnkB variants have altered cellular function, and are associated with ASD, epilepsy, and AnkB syndrome (Rubeis et al. 2014; Iossifov et al. 2014; Guo et al. 2017; Swayne et al. 2017). Whether AnkB variants affect its regulation of Cav2.1 had not previously been investigated. Therefore, based on these previous findings and related knowledge gaps, I formulated the following hypotheses:

1. AnkB regulates Cav2.1 expression levels and/or localization
2. AnkB's impact on Cav2.1 is perturbed by AnkB mutations

In order to investigate these hypotheses, I formulated the following two related aims.

Aim 1: Determine if AnkB and AnkB variants alter surface localization of Cav2.1

In Aim 1, I use cell surface biotinylation to investigate the localization of Cav2.1 in the presence of wildtype AnkB and three AnkB variants, p.S646F, p.Q879R, and p.E1458G in HEK293T cells. Furthermore, I investigate if Cav accessory subunits have

an effect on AnkB and Cav2.1 localization. Also, I investigate the effect of wildtype or variant AnkB on overall expression and binding affinity.

Aim 2: Determine the effect of partial AnkB deletion on synaptic expression of Cav2.1

In Aim 2, I investigate the localization of Cav2.1 to the synapse in mouse cortex. I prepared synaptosomes from conditional heterozygous AnkB knockout mouse to observe the effect of partial loss of AnkB on Cav2.1 levels in synaptosomal fraction.

2. Ankyrin B and Ankyrin B variants modulate intracellular Cav2.1 levels

This chapter is written as a manuscript that we have submitted for publication.

Catherine S.W. Choi[1], Ivana A. Souza[2], Juan C. Sanchez-Arias[1], Gerald W. Zamponi[2], Laura T. Arbour[1,3], and Leigh Anne Swayne[1*]

1. Division of Medical Sciences, University of Victoria, Victoria, British Columbia

2. Department of Physiology and Pharmacology , Hotchkiss Brain Institute and Alberta Children's Hospital Research Institute, Cumming School of Medicine, University of Calgary, Calgary, Alberta

3. Department of Medical Genetics, University of British Columbia, Vancouver, British Columbia

KEYWORDS

Ankyrin B, Cav2.1, CACNA1A, intracellular pool, surface localization, synapse

Authors' contributions

CSWC and LAS designed the research project with input from all authors. CSWC performed the majority of the experiments. IAS performed the electrophysiology experiment, and JCSA aided in mouse tissue collection. CSWC and LAS wrote the manuscript. CSWC, LAS, IAS, JCSA, LTA, and GWZ revised the manuscript.

2.1 Abstract

Ankyrin B (AnkB) is an adaptor and scaffold for motor proteins and various ion channels that is ubiquitously expressed, including in the brain. AnkB has been associated with neurological disorders such as epilepsy and autism spectrum disorder, but understanding of the underlying mechanisms is limited. Cav2.1, the pore-forming subunit of P/Q type voltage gated calcium channels, is a known interactor of AnkB and plays a crucial role in neuronal function. Here we discovered that AnkB increases overall Cav2.1 levels without impacting surface Cav2.1 levels in HEK293T cells. An AnkB variant, p.S646F, which we recently discovered to be associated with seizures, further increases overall Cav2.1 levels, again with no impact on surface Cav2.1 levels. In addition, we found that partial deletion of AnkB in cortex results in a decrease in overall Cav2.1 levels, with no change to the levels of Cav2.1 detected in synaptosome fractions. Our work suggests that AnkB regulates an intracellular pool of Cav2.1 and that this increase is further augmented with expression of the AnkB variant associated with seizure (AnkB p.S646F). These novel findings have important implications for understanding the role of AnkB and Cav2.1 in the regulation of neuronal function in health and disease.

2.2 Introduction

Ankyrin B (AnkB) is a scaffolding adaptor protein that plays a variety of roles in multiple systems including the brain, heart, and pancreas (Scotland et al. 1998; Smith & Penzes 2018; Bennett & Healy 2009; Peter J Mohler et al. 2007; Koenig & Mohler 2017; Lorenzo et al. 2015). In neurons, it can serve as an adaptor for the dynactin complex and phosphoinositide 3-phosphate vesicles, and serves as a scaffold for multiple ion channels including Na^+/K^+ ATPase (NKA), Na^+/Ca^{2+} exchanger type 1 (NCX1) , inositol-trisphosphate receptor type 1 (IP3R), and T-type voltage gated calcium channels (VGCC) to the spectrin cytoskeleton network (Lorenzo et al. 2014; Lencesova et al. 2004; Mohler et al. 2005; Garcia-Caballero et al. 2018). In humans, AnkB variants can lead to AnkB syndrome, characterized by a spectrum of cardiac dysfunction (Mohler et al. 2004; Peter J. Mohler, Le Scouarnec, Denjoy, Lowe, Guicheney, Caron, Driskell, J. J. Schott, et al. 2007). AnkB has also been associated with neurological disorders such as autism spectrum disorder and epilepsy (Iossifov et al. 2014; Rubeis et al. 2014; Guo et al. 2017). A recent study by our group identified a genetic variant resulting in an amino acid substitution in the membrane binding domain, AnkB p.S646F, that is associated with seizures in addition to cardiac symptoms (Swayne et al. 2017). The putative molecular and cellular mechanisms underlying neurological symptoms associated with AnkB variants are unknown.

AnkB interacts with Cav2.1, the pore-forming subunit of P/Q type VGCCs, in brain tissues isolated from adult mice (Kline et al. 2014). Cav2.1 is detected pre- and post- synaptically, with multiple isoforms (ranging from 160-230 kDa, including a 190 kDa dominant isoform) expressed in brain (Fu et al. 2017; Sakurai et al. 1996). Cav2.1

plays a role in calcium-triggered neurotransmitter release at the presynaptic membrane, where it interacts with vesicle fusion machinery proteins, such as syntaxin 1A (Rettig et al. 1996; Catterall 2011; He et al. 2018). Cav2.1 is also found at the postsynaptic density where it interacts with AMPA receptors (Kang et al. 2006). Additionally, Cav2.1 is present on intracellular membranes and is crucial for the fusion of lysosome to endosomes and autophagosomes (Tian et al. 2015). Cav2.1 loss of function mutations leads to disorders including episodic ataxia as well as cognitive impairment and epilepsy (Damaj et al. 2015; Heyne et al. 2018). In contrast, a gain of Cav2.1 function is associated with forms of familial migraine, altogether demonstrating the importance of this channel for proper neurological function (Pietrobon 2010).

Considering the interaction between Cav2.1 and AnkB and the overlap in neurological disorders caused by variants in their genes, we decided to explore the relationship between Cav2.1 and AnkB at the subcellular level using transient expression in HEK293T cells and cortex-specific AnkB conditional knockout mice. We found that AnkB p.S646F increased overall Cav2.1 expression levels, but did not change the binding affinity or surface Cav2.1 levels in HEK293T cells. In the mouse cortex, we observed that overall AnkB and Cav2.1 expression levels increased during early postnatal development. Focusing on the synaptic compartment in juvenile mice (postnatal day 30), glutamatergic-neuron-specific heterozygous AnkB KO led to a decrease in overall Cav2.1 expression levels but no change in synaptosome fraction levels. Our work suggests that AnkB plays a role in regulating Cav2.1 intracellular pools but not synaptosomal or surface localization.

2.3 Methods

2.3.1 Plasmids

Wildtype *ANK2* (NCBI accession number NM_020977.3), subcloned into pAcGFP backbone (c-terminal tag), encodes for the 220 kDa AnkB isoform. *ANK2* c.1937C>T (p.S646F), c.2636A>G (p.Q879R), and c.4373A>G (p.E1458G) point mutations of AnkB-GFP were created using QuikChange II site-directed mutagenesis (Agilent). Created plasmids were confirmed by DNA sequencing of the entire coding sequence (Eurofins Genomics). *CACNA1A* (Cav2.1) (NM_012918.3), *CACNA2D1* ($\alpha_2\delta_1$) (NM_012919.3), and *CACNB4* (β_4) (NM_001105733.1) in pcDNA3.1 plasmid were a kind gift from Dr. Terry Snutch (University of British Columbia) (Snutch et al. 1990).

2.3.2 Cell culture and transfection

Human Embryonic Kidney 293T (HEK293T) cells from American Type Culture Collection were cultured in Dulbecco's modified Eagle's medium supplemented with 10 % fetal bovine serum, 100 U/mL penicillin, and 100 μg/mL streptomycin (all from Gibco/Thermo Fisher Scientific). Cells were transfected with 7.5 mM linear polyethylenamine (Polysciences) at a ratio of 1 μg of DNA to 10 μL of PEI, and collected 48 hr post-transfection.

2.3.3 Protein lysate and analysis

HEK293T were washed twice in PBS before addition of cell lysis buffer (25 mM Tris-HCl, 150 mM NaCl, 1 mM EDTA, 1 % IGEPAL CA-630, 5 % glycerol) supplemented with 10 μL/mL of protease inhibitor cocktail (Millipore Sigma), 0.2 mM PMSF, and 10 μM sodium orthovanadate. Whole cortex, whole hippocampus, or whole cerebellum from C57BL/6J mice were homogenized in brain lysis buffer (9.1 mM

Na_2HPO_4, 1.7 mM NaH_2PO_4, 150 mM NaCl, 1 % IGEPAL CA-630, 0.5 % sodium deoxycholate, 0.1 % sodium dodecyl sulfate) with the same supplements. Lysate was incubated on ice for 30 min and then centrifuged at 12,000 rpm for 20 min. Supernatants were collected and used for analysis. HEK293T lysates were mixed with sample buffer and reducing agents and stored at -80^{o}C before running on SDS-PAGE gel. Brain samples with sample buffer and reducing agents were heated to 70^{o}C for 10 min. Either homemade SDS-PAGE or TGX Stain-Free^{TM} (Bio-Rad) gels was used and transferred overnight onto 0.2 μm pore-size PVDF membrane (Bio-Rad) for Western blotting. Membranes were blocked with 5 % skim milk in PBS with 0.1 % Tween-20, and probed with primary antibodies. Blots were quantified using ImageJ (http://imagej.nih.gov/ij/).

2.3.4 GFP immunoprecipitation

GFP Dynabeads^{TM} were prepared by adding 2.5 μg of anti-GFP mouse monoclonal antibody (Roche/Millipore Sigma) to 25 μL of Dynabeads^{TM} Protein G (Invitrogen/Thermo Fisher Scientific) in PBS-T (2.7 mM KCl, 10 mM NaH_2PO_4, 1.8 mM KH_2PO_4, 137 mM NaCl, 0.02% Tween 20) and incubated at room temperature on a rotator for 30 min. Beads were washed 2x in conjugation buffer (20 mM sodium phosphate (pH 7.4), 150 mM NaCl), cross-linked by resuspending in 5 mM of BS^3 (Thermo Fisher Scientific) in conjugation buffer, and incubated at room temperature on a rotator for 30 min. Reaction was quenched by adding Tris-HCl (pH 7.5) to a final concentration of 50 mM and incubated at room temperature on a rotator for 15 min. Beads were washed 3x in PBS-T. HEK293T lysates were added to the washed beads and incubated at 4^{o}C for 2 hr on a rotator. Beads were then washed 3x in cell lysis buffer, eluted in 1x sample buffer, and stored at -80^{o}C before running on SDS-PAGE gel.

2.3.5 Endogenous immunoprecipitation

As with GFP immunoprecipitation, Dynabeads™ were prepared by adding anti-AnkB antibody (Thermo Fisher Scientific) or mIgG (Jackson ImmunoResearch) to Dynabeads™ at a ratio of 1 μg of antibody to 10 μL of dynabeads™. Mouse cortex was homogenized in IP buffer (9.1 mM Na_2HPO_4, 1.7 mM NaH_2PO_4, 150 mM NaCl, 0.32 M sucrose, 2 mM EDTA, 0.1 % Triton X-100, 0.1% sodium deoxycholate, and 0.1% sodium dodecyl sulfate). Cortex lysates were precleared by incubating with 75 μL of mIgG-Dynabeads™ for 1 hr at 4°C on a rotator. Lysates were removed from the mIgG-Dynabeads™ and added to either 40μL of AnkB- or mIgG- Dynabeads™ and incubated for 2 hr at 4°C on a rotator. Beads were then washed 3x with IP buffer, eluted with 1x sample buffer with reducing agents and heated at 70°C for 10min before running on SDS-PAGE gel.

2.3.6 Cell surface biotinylation

Transfected HEK293T cells were washed twice with biotinylation buffer (137 mM NaCl, 2.7 mM KCl, 1.8 mM KH_2PO_4, 10 mM Na_2HPO_4, 0.5 mM $MgCl_2$, 1 mM $CaCl_2$) and incubated in biontinylation buffer with and without 0.25 mg/mL EZ-Link™ Sulfo-NHS-SS-Biotin (Thermo Fisher Scientific) for 30 min at 4°C on a rocker. Biotinylation reaction was quenched by adding glycine to the plate to a final concentration of 100 mM (quenching buffer). Cells were then washed twice and then incubated with quenching buffer for 15 min at 4°C. Cells were then lysed in TBS lysis buffer (50 mM Tris, 150 mM NaCl, 1% IGEPAL CA-630), incubated on ice for 30 min, and spun at 12,000 rpm for 20 min. Lysate was preclear in 50 μL of iminobiotin agarose beads (Pierce/Thermo Fisher Scientific) for 1 hr at 4°C on rotator. Precleared lysate was

then added to 50 µL of NeutrAvidin™ agarose beads (Pierce/Thermo Fisher Scientific) for 2 hr at 4°C on rotator. Beads were then washed 4x with TBS lysis buffer, 4x with high salt TBS lysis buffer (50 mM Tris, 300 mM NaCl, 1% IGEPAL CA-630), and finally 2x in 50 mM Tris. Beads were eluted by incubating in 1x sample buffer with reducing agents and stored at -80°C before running on SDS-PAGE.

2.3.7 Electrophysiology

Whole cell patch clamp recordings were performed 72 hr after transfection using an Axopatch 200B amplifier linked to a computer with pCLAMP 9.2 software. Currents were recorded using the external solution (5 mM $BaCl_2$, 137.5 mM CsCl, 1 mM $MgCl_2$, 10 mM HEPES and 10 mM Glucose, pH 7.4) and internal pipette solution (130 mM CsCl, 2.5 mM $MgCl_2$, 10 mM HEPES, 5 mM EGTA, 3 mM ATP, 0.5 mM GTP, pH 7.4). The current/voltage (I/V) relationship was obtained by applying 250 ms pulses from a holding potential of -100 mV. Test pulses ranged from -50 mV to +50 mV in 5 mV increments. Current density was determined by dividing the peak current by whole cell capacitance and the I/V currents were fitted with a modified Boltzmann equation: $I = G_{max} \times (V_m - V_r)/(1 + \exp(-(V_m - V_{1/2})/k))$, where I is the peak current, V_m is the membrane potential, $V_{1/2}$ is the voltage for half activation, V_r is the reversal potential, and k is the slope factor. Data were analyzed using the Clampfit 10.3 software (Molecular Devices).

2.3.8 Experimental Animals

The animal protocol was approved and the experiments were performed in accordance to the ethical standards set by the University of Victoria's Animal Care Committee. $AnkB^{flox/flox}$ mice were a kind gift from Dr. Peter Mohler (Ohio State

University) and were back-crossed in-house for 5 generations onto a C57BL/6J background (000664, The Jackson Laboratory) (Smith et al. 2015). AnkB$^{flox/wt}$ were crossed with Emx1$^{IRES-cre}$ (#005628, The Jackson Laboratory) to generate control (CTL; AnkB$^{wt/wt}$: Emx1$^{IRES-cre}$) and conditional heterozygous knockout (AnkB$^{glut+/-}$; AnkB$^{flox/wt}$: Emx1$^{IRES-cre}$) littermates. This Emx1$^{IRES-cre}$ drives recombination in cells that give rise to excitatory neurons and glia of the cerebral cortex and recombination has been shown to occur as early as embryonic day 10.5 (Gorski et al. 2002). Male and female mice were used in the present study; weaning was carried out at postnatal day 21. All animals were housed under a 12-hour light/dark cycle with water and food *ad libitum*.

2.3.9 Synaptosome preparations

Synaptosomes were prepared as previously described (Sanchez-arias et al. 2019). Briefly, P14 and P30 cortices were homogenized in Syn-PER^{TM} (Thermo Fisher Scientific) and a small fraction was saved for analysis. The homogenate was spun at 1,200 g for 10 min. The supernatant was transferred to a new tube and spun at 15,000 g for 20 min. The synaptosome pellet was washed by resuspending with Syn- PER^{TM} with 5% DMSO. Sample was stored at -80^{o}C until needed. Frozen synaptosomes were thawed and spun again at 15,000 g for 20 min. The pellet was then resuspended in Syn-PER^{TM}, mixed with sample buffer and reducing agents, heated to 70^{o}C for 10 min, and analyzed by SDS-PAGE.

2.3.10 Antibodies

Primary antibodies used include anti-Cav2.1 (1:500, Alomone Labs), anti-GFP rabbit polyclonal (1:2000, Invitrogen/Thermo Fisher Scientific), anti-GAPDH (1:3000, Novus Biologicals), anti-transferrin receptor (1:1000, Invitrogen/Thermo Scientific), anti-

CACNA2D1 (1:1000, Abcam), anti-AnkB (1:500, Thermo Fisher Scientific), and anti-syntaxin 1A (1:5000, Millipore Sigma). Secondary antibodies used include horseradish peroxidase (HRP)-conjugated AffiniPure anti-rabbit immunoglobulin and anti-mouse IgG (all at 1:4000; Jackson ImmunoResearch).

2.3.11 Statistical Analysis

Bar graphs display means with standard error of the mean. Analysis used either one-way or two way ANOVA as appropriate. Corrections for multiple comparisons are indicated in figure legends. Data was analyzed using GraphPad Prism version 6.01, with significance denoted as $p < 0.05$ (*), $p < 0.01$ (**), $p < 0.001$ (***), and $p < 0.0001$ (****).

2.4 Results

2.4.1 Wildtype AnkB and AnkB variants increase overall Cav2.1 expression levels in HEK293T cells

We first investigated the impact of AnkB expression on overall Cav2.1 expression levels. We performed Western blotting with lysates from HEK293T cells transiently co-expressing Cav2.1 along with wildtype AnkB-GFP or AnkB p.S646F, and two other AnkB variants, p.Q879R and p.E1458G (Fig. 1a). The human variant AnkB p.Q879R was selected for comparison, because the mutation resides within the linker region required for proper AnkB localization (He et al. 2013; Exome variant server NHLBI 2019). In addition, AnkB p.E1458G (referred to as E1425G in previous literature) was selected for its well-characterized cardiac abnormalities as well as loss of binding to NKA, NCX1, and IP3R (Mohler et al. 2003; Mohler et al. 2005). Overall Cav2.1 levels

increased significantly in cells co-expressing wildtype AnkB-GFP (Fig. 1aii). This effect of AnkB on Cav2.1 levels was even greater in AnkB p.S646F-expressing cells, and cells expressing the other two variants revealed similar effects on Cav2.1 (albeit with differences in statistical significance), suggesting Cav2.1 levels are up-regulated by expression of AnkB as well as its variants. It is important to note that wildtype AnkB-GFP and AnkB-GFP variants were expressed at similar levels (Fig. 1aiii).

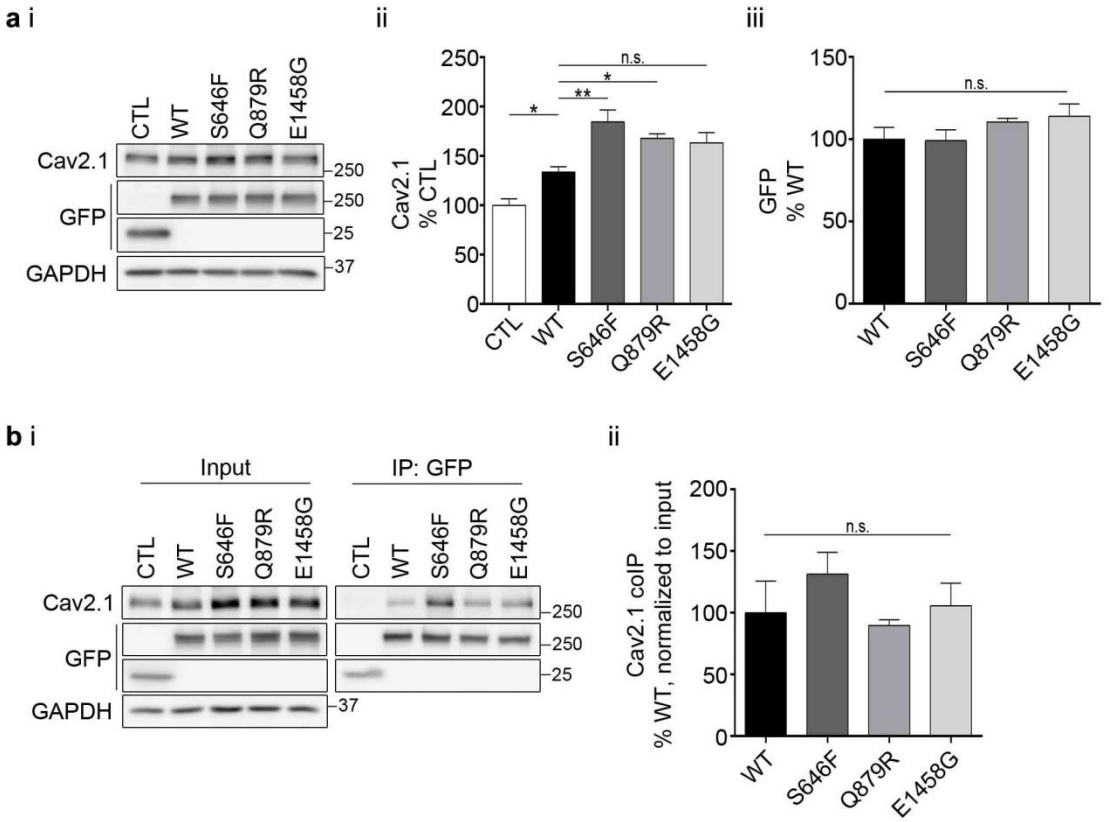

Figure 2.1 AnkB mutations increased expression of Cav2.1 without altering its binding affinity

(ai) Representative Western blots of whole cell lysates of HEK293T cells transfected with Cav2.1 and GFP control or wildtype or mutant AnkB-GFP. (aii) Quantification of Cav2.1 normalized to GAPDH and expressed as a percentage of control (CTL). One-way

ANOVA followed by Sidak's multiple comparison, $N = 5$, $F_{(4,20)} = 15.59$, $p < 0.0001$. (aiii) Quantification of GFP normalized to GAPDH and expressed as a percentage of wildtype. One-way ANOVA, $N = 5$, $F_{(3,16)} = 1.408$, $p = 0.2770$. (bi) Representative co-IP Western blots of transfected HEK293T cells. (bii) Quantification of Cav2.1 co-IP normalized to GFP IP and Cav2.1 input and expressed as a percentage of wildtype. One-way ANOVA, $N = 3$, $F_{(3,8)} = 0.9381$, $p = 0.4662$.

2.4.2 AnkB variants do not alter AnkB-Cav2.1 binding affinity

To investigate whether the increase in overall Cav2.1 expression levels observed with AnkB variants was due to changes in binding affinity by AnkB mutations, we immunoprecipitated GFP from HEK293T cells co-expressing Cav2.1 and wildtype AnkB-GFP or an AnkB-GFP variants (Fig. 1b). The quantity of Cav2.1 co-immunoprecipitating with AnkB-GFP or its variants corresponded closely with the overall expression levels in whole cell lysates. As such, no significant differences in co-precipitation of Cav2.1 was observed following normalization to Cav2.1 input levels (Fig. 1bii), suggesting AnkB p.S646F nor any of the other variants altered the AnkB-Cav2.1 binding affinity.

2.4.3 Wildtype AnkB and AnkB variants differentially impact cell surface Cav2.1 levels

To determine if the increase in Cav2.1 expression by AnkB led to an increase in cell surface expression, we performed cell surface biotinylation in HEK293T cells transiently expressing Cav2.1 and GFP control, wildtype, or mutant AnkB-GFP. Although AnkB-GFP increased overall Cav2.1 expression levels (Fig. 1a), surprisingly, it did not impact surface Cav2.1 levels (Fig. 2a). Similarly, AnkB p.S646F and AnkB

p.Q879R had no significant effect on surface Cav2.1 levels. Conversely, AnkB p.E1458G led to a slight decrease in surface Cav2.1 levels. In addition, we were able to capture cytoplasmic proteins co-precipitating with surface proteins, including a pool of surface-associated AnkB-GFP, by using a gentle lysis buffer in our cell surface biotinylation protocol. We detected a surface associated pool of wildtype AnkB-GFP; however, none of the AnkB variants exhibited a significant surface-associated pool.

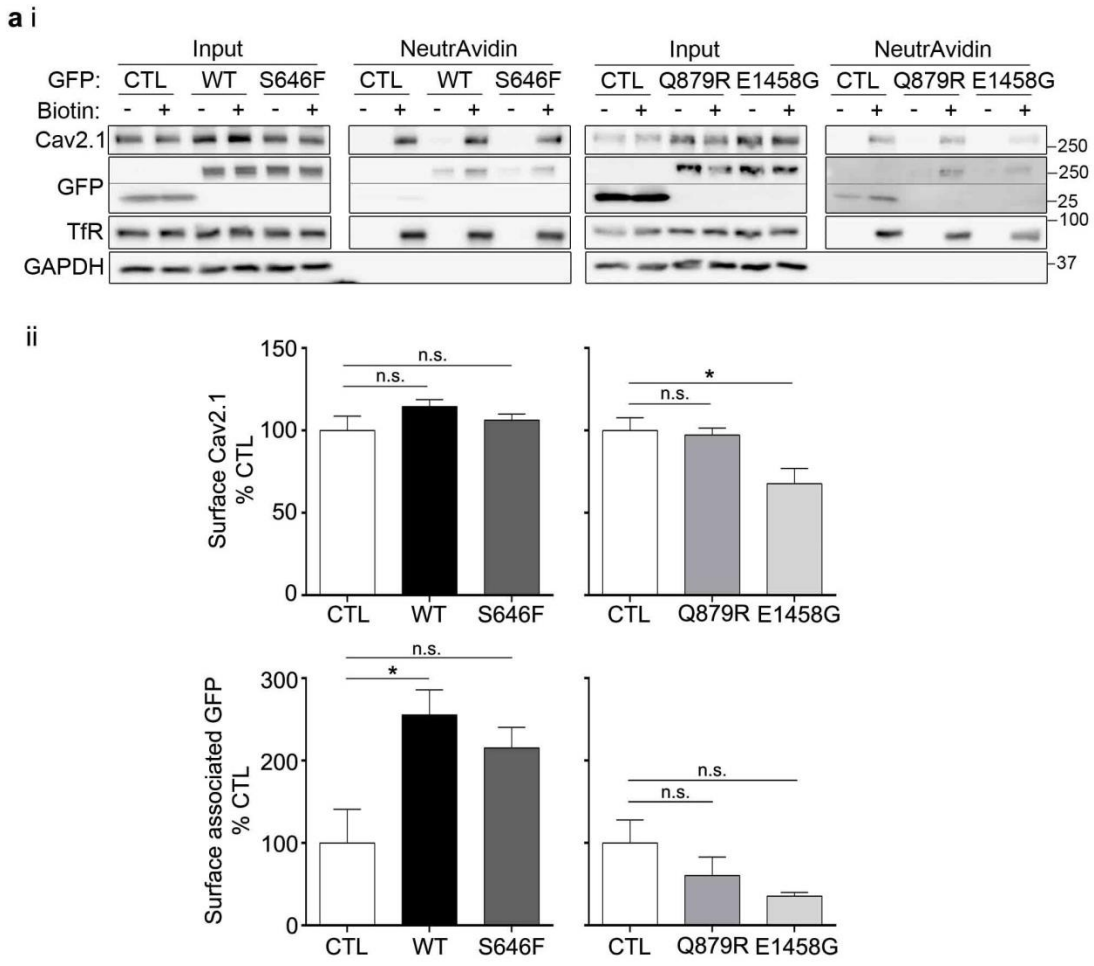

Figure 2.2 AnkB wildtype, p.S646F and p.Q879R do not impact Cav2.1 surface expression in HEK293T cells in the absence of auxiliary subunits.

(ai) Representative surface biotinylation Western blots of inputs and NeutrAvidin surface fraction. GAPDH was used as a negative control to ensure intracellular proteins were not biotinylated. Transferrin receptor (TfR) served as a positive pulldown control, (aii) Quantification of surface proteins normalized to surface TfR and expressed as a percentage of GFP control (CTL). One-way ANOVA followed by Dunnett's multiple comparison, N = 3-4, $F_{(2,8)} = 1.222$, $p = 0.3443$ (Cav2.1: WT,S646F); $N = 3$, $F_{(2,6)} = 5.891$, $p = 0.0384$ (Cav2.1: Q879R, E1458G); $N = 3$, $F_{(2,6)} = 5.764$, $p = 0.0282$ (GFP: WT, S646F); $N = 3$, $F_{(2,6)} = 2.393$, $p = 0.1721$ (GFP: Q879R, E1458G).

2.4.4 AnkB variants modulate crosstalk between AnkB, Cav2.1, and accessory subunits

Trafficking and regulation of Cav2.1 is affected by accessory $\alpha_2\delta$ and β subunits, which affect expression levels, ER exit, and surface localization of the pore-forming Cav subunit (Weiss & Zamponi 2017; Buraei & Yang 2010). To determine if these accessory subunits impact AnkB regulation of overall and surface Cav2.1expression levels, we performed surface biotinylation on HEK293T expressing AnkB, Cav2.1 as well as $\alpha_2\delta_1$ and β_4. There was still no effect of wildtype AnkB or AnkB p.S646F on surface Cav2.1 expression levels in the presence of $\alpha_2\delta_1$ and β_4 (Fig. 3a). Conversely, AnkB p.Q879R increased Cav2.1 surface levels in the presence of $\alpha_2\delta_1$ and β_4. Moreover, $\alpha_2\delta_1$ and β_4 expression promoted surface-association of AnkB p.S646F and p.Q879R variants, which did not occur in the absence of accessory subunits. Furthermore, wildtype AnkB increased $\alpha_2\delta_1$ surface levels, whereas AnkB variants did not. Together these results suggest that AnkB variants modulate crosstalk between AnkB, Cav2.1 and accessory subunits.

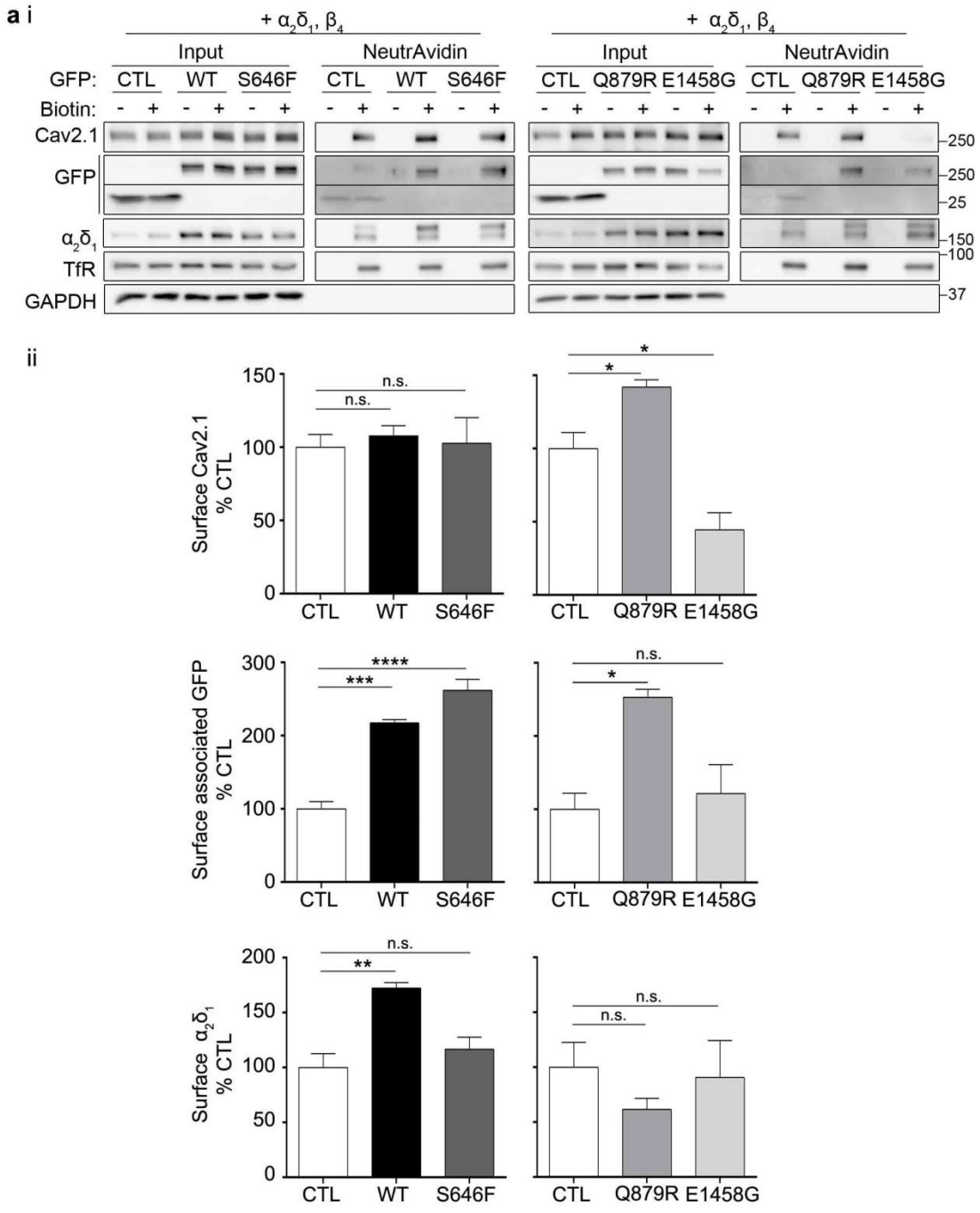

Figure 2.3. AnkB and its variants differentially impact Cav2.1 surface expression in HEK293T cells in the presence of auxiliary subunits (α2δ1 and β4).

(ai) Representative surface biotinylation Western blots of inputs and surface fraction. (aii) Quantification of surface proteins normalized to surface TfR and expressed as a

percentage of GFP control (CTL). One-way ANOVA followed by Dunnett's multiple comparison, $N = 3$, $F_{(2,6)} = 0.1117$, $p = 0.8961$ (Cav2.1: WT,S646F); $N = 3$, $F_{(2,6)} = 25.14$, $p = 0.0012$ (Cav2.1: Q879R, E1458G); $N = 3$, $F_{(2,6)} = 59.18$, $p = 0.0001$ (GFP: WT,S646F); $N = 3$, $F_{(2,6)} = 9.587$, $p = 0.0135$ (GFP: Q879R, E1458G); $N = 3$, $F_{(2,6)} = 14.18$, $p = 0.0053$ (α2δ1: WT,S646F); $N = 3$, $F_{(2,6)} = 0.6860$, $p = 0.5392$ ($\alpha_2\delta_1$: Q879R, E1458G).

2.4.5 AnkB and AnkB variants increase Cav2.1-based VGCC peak current density

We next investigated the impact of wildtype AnkB and AnkB variants on Cav2.1-based VGCC properties. We measured peak current density using whole-cell patch clamp in HEK293T cells expressing wildtype AnkB-GFP or AnkB-GFP variants along with Cav2.1, and accessory subunits ($\alpha_2\delta_1$ and β_4). Expression of wildtype AnkB and AnkB variants all resulted in an increase in peak current density, with the greatest increase by AnkB p.Q879R (Fig. 4a). Neither wildtype nor mutant AnkB significantly affected the voltage dependence of activation of Cav2.1 channels (Fig. 4b).

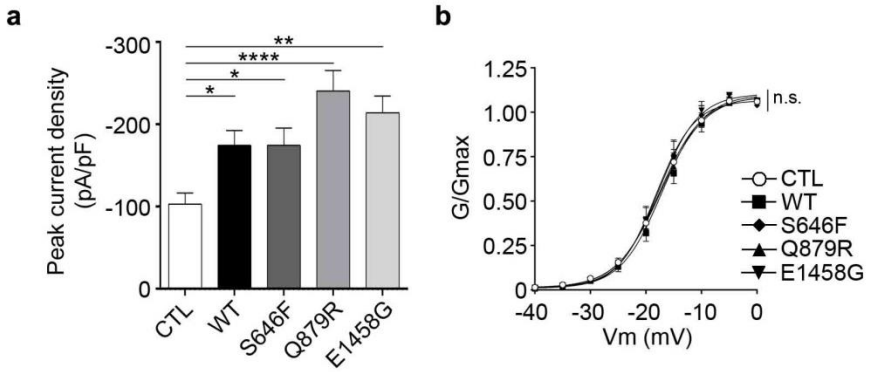

Figure 2.4 AnkB and its variants increase peak current density but did not alter activation kinetics in HEK293T cells co-transfected with Cav2.1, $\alpha_2\delta_1$, β_4, and GFP control, wildtype, or mutant AnkB-GFP.

(a) Peak current density was determined by dividing the peak current by whole cell capacitance. One-way ANOVA followed by Dunnett's multiple comparison, $F_{(4,151)} = 6.465$, $p < 0.0001$ (b) Normalized G/Gmax vs. voltage curve fitted using Boltzmann's equation. One-way ANOVA $F_{(4, 50)} = 0.0022$, $p > 0.9999$

2.4.6 AnkB alters a non-synaptic pool of Cav2.1

To further investigate the role of AnkB in the regulation of Cav2.1 expression in mouse brain, we first determined their postnatal developmental expression profiles from postnatal day 7 (P7) to P60 in wildtype mice (Fig. 5a). In the cortex and hippocampus, both AnkB and Cav2.1 expression levels increased markedly between P7 and P14. Conversely, in the cerebellum, AnkB levels increased gradually over postnatal development, while Cav2.1 levels were high from P7 onwards. Cav2.1 is known to interact with AnkB in adult mouse cortex (Kline et al. 2014). To determine whether Cav2.1 and AnkB also interact during early postnatal development, we immunoprecipitated AnkB from P14 wildtype mouse cortex (Fig. 5b). Our results confirmed that AnkB interacts with Cav2.1 in P14 mouse cortex. We also examined syntaxin 1A, an important SNARE protein that interacts with the *syn*aptic *pr*otein *int*eraction (synprint) site within the Cav2.1 II-III linker which is also the locus of the AnkB interaction (Rettig et al. 1996; Kline et al. 2014), and discovered that syntaxin 1A was also immunoprecipitated by AnkB.

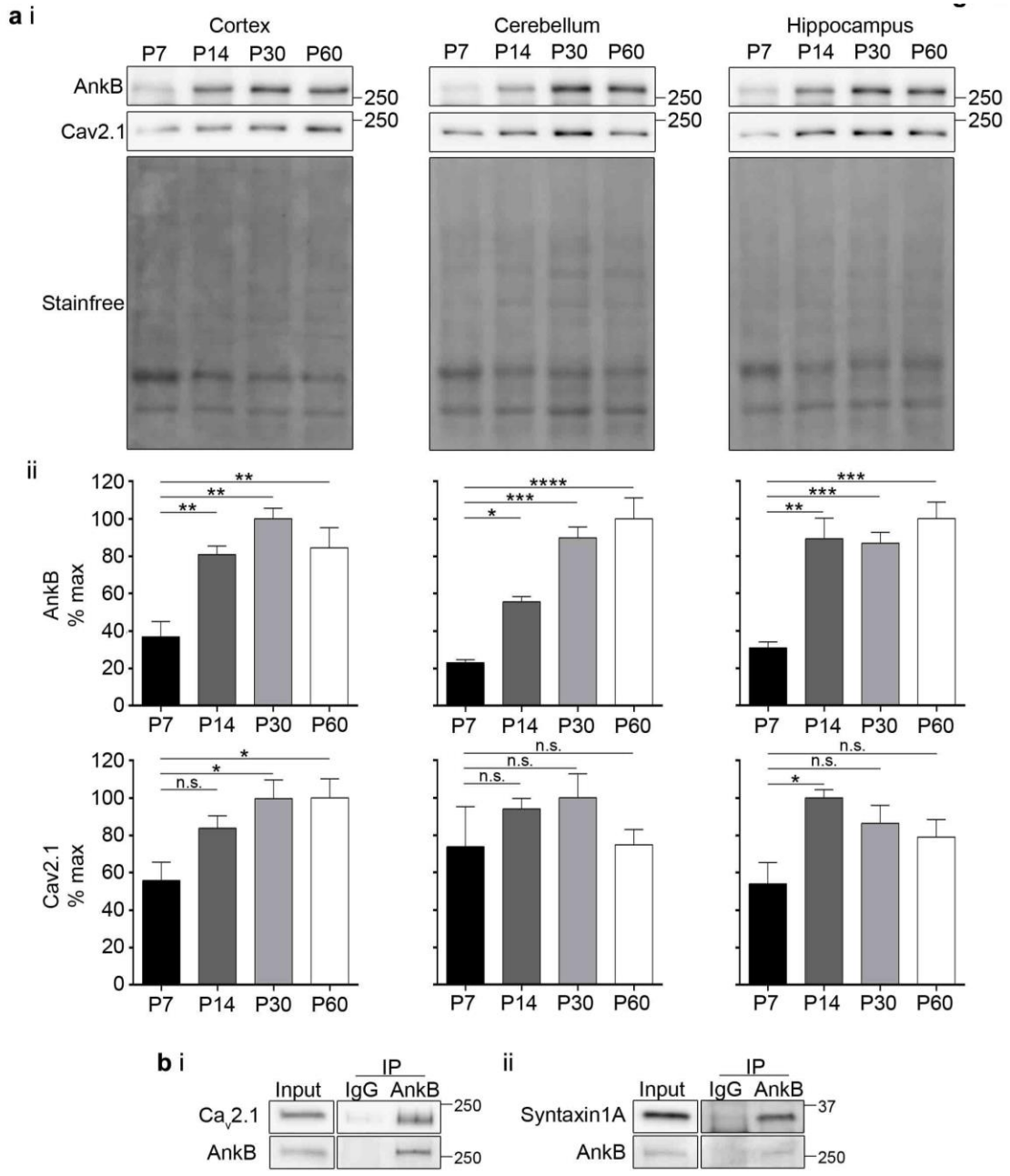

Figure 2.5 Both AnkB and Cav2.1 show similar increase in expression during early cortical development.

(ai) Representative Western blots of AnkB and Cav2.1 in mice cortex, hippocampus, and cerebellum from P7 to P60. (aii) Quantification of AnkB and Cav2.1 normalized to stain-free. One-way ANOVA followed by Dunnett's multiple comparison, $N = 3$, $F_{(3,8)} =$

12.52, $p = 0.0022$ (cortex, AnkB); $F_{(3,8)} = 4.945$, $p = 0.0314$ (cortex, Cav2.1); $F_{(3,8)} = 28.89$, $p = 0.0001$ (cerebellum, AnkB); $F_{(3,8)} = 0.9790$, $p = 0.4494$ (cerebellum, Cav2.1); $F_{(3,8)} = 15.70$, $p = 0.0010$ (hippocampus, AnkB); $F_{(3,8)} = 4.507$, $p = 0.0393$ (hippocampus, Cav2.1). (bi-ii) Representative Western blots of inputs and control IgG or AnkB immunoprecipitation from P14 mouse cortex. $N = 3$.

Based on the coordinated developmental increase in AnkB and Cav2.1 levels and the early postnatal AnkB-Cav2.1 interaction, we next investigated the impact of AnkB KO on Cav2.1 levels in cortical tissue. To do this we used cortical tissue isolated from control mouse (CTL; $AnkB^{wt/wt}$: $Emx1^{IRES\text{-}cre}$) and AnkB conditional heterozygous knockout ($AnkB^{glut+/-}$; $AnkB^{flox/wt}$: $Emx1^{IRES\text{-}cre}$) littermates and performed synaptosome fractionation (Fig. 6a) yielding homogenates (H; consisting of whole cortical lysate) and synaptosomes (Syn). Confirming successful partial deletion of *ANK2*, AnkB levels were lower in $AnkB^{glut+/-}$ than control cortical tissue homogenate (Fig. 6b). We validated synaptic compartment enrichment in the synaptosome fractions using an antibody against post-synaptic density protein 95 (PSD95), a key excitatory post-synaptic scaffold (El-Husseini et al. 2000). We compared Cav2.1 expression in synaptosome and homogenate fractions from P14 and P30 cortices using Western blot analysis. The levels of AnkB and Cav2.1 were enriched in control and $AnkB^{glut+/-}$ synaptosome fractions at P14 and P30, confirming localization to synaptic compartments (Fig. 6c)(Collins et al. 2006; Jordan et al. 2004; Peng et al. 2004; Fu et al. 2017). AnkB levels were lower in $AnkB^{glut+/-}$ synaptosomes than control synaptosomes, whereas Cav2.1 levels were unchanged, suggesting that the Cav2.1 synaptic pool remained unaffected. However, Cav2.1 cortical homogenate expression levels were lower in $AnkB^{glut+/-}$ than control at P30. We also

investigated the consequences of partial AnkB KO on the expression levels of syntaxin 1A. Similarly, syntaxin 1A cortical homogenate expression levels from P30 AnkB$^{glut+/-}$ were lower than control, whereas there was no change in syntaxin 1A synaptosome levels between groups. These decreases in Cav2.1 and syntaxin 1A expression were only seen at P30 but not at P14. Unlike Cav2.1 or syntaxin 1A, AnkB$^{glut+/-}$ led to a higher level of PSD95 in P30 synaptosome than wildtype control.

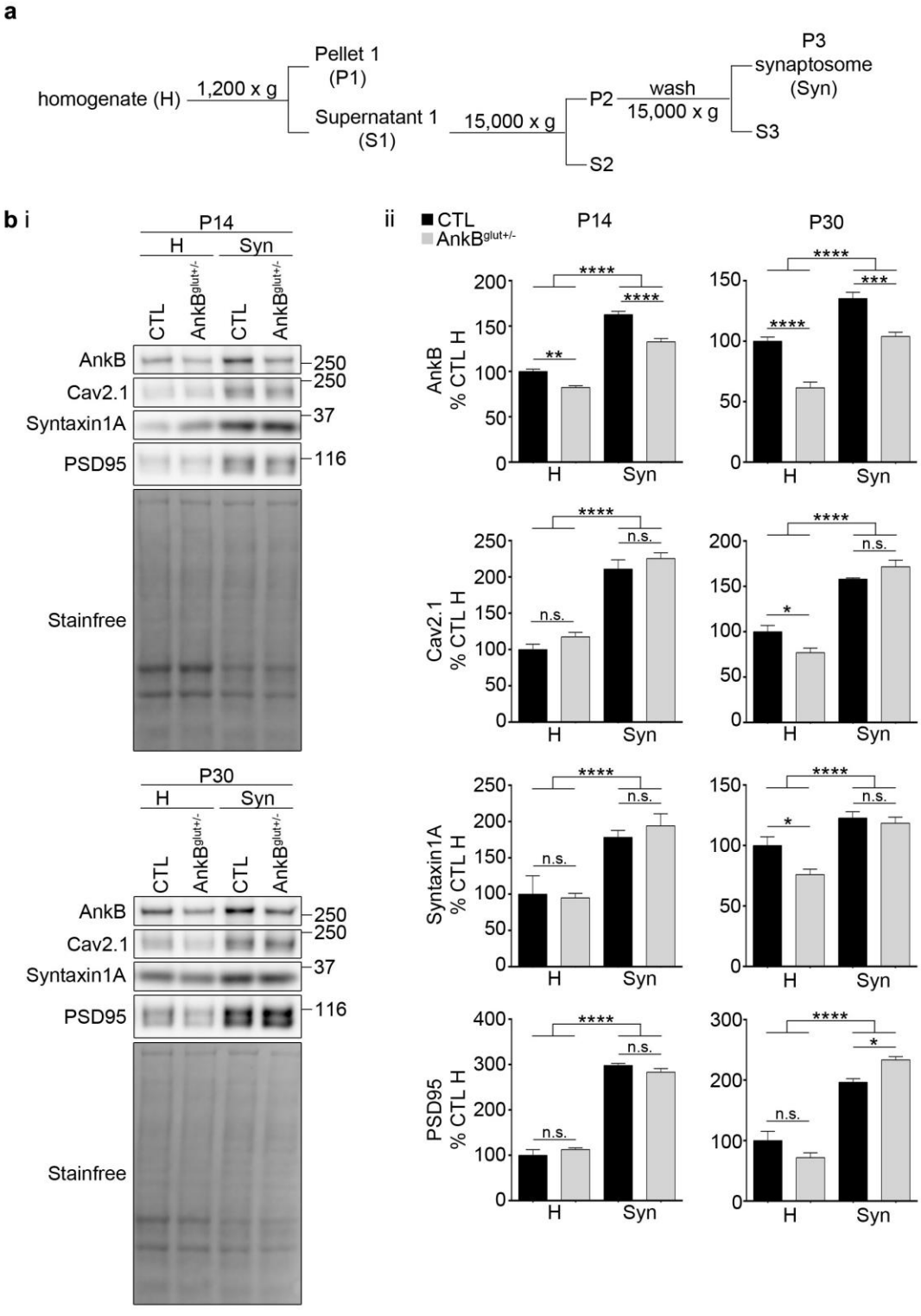
a
homogenate (H)
1,200 x g
Pellet 1 (P1)
Supernatant 1 (S1)
15,000 x g
P2
wash 15,000 x g
P3 synaptosome (Syn)
S3
S2
b i
P14
H
Syn
CTL
AnkBglut+/-
AnkB
Cav2.1
Syntaxin1A
PSD95
Stainfree
250
250
37
116
P30
ii
CTL
AnkBglut+/-
P14
P30
AnkB % CTL H
Cav2.1 % CTL H
Syntaxin1A % CTL H
PSD95 % CTL H
****
***
**
*
n.s.
H
Syn

Figure 2.6 Cav2.1 expression levels are decreased in whole cortex homogenate of P30 glutamatergic-neuron-specific heterozygous AnkB KO mice but does not change in synaptosomal preparations.

(a) Flow chart of synaptosome preparation procedure. (bi) Representative Western blots of P14 and P30 homogenate (H) and synaptosome (Syn) fraction from control (CTL; $AnkB^{wt/wt}$: $Emx1^{IRES\text{-}cre}$) and AnkB conditional heterozygous knockout ($AnkB^{glut+/-}$; $AnkB^{flox/wt}$: $Emx1^{IRES\text{-}cre}$) cortices. (bii) Quantification of immunoblots normalized to stain-free and expressed as a percentage of control homogenate. Two-way ANOVA followed by Sidak's multiple comparison, $N = 5$, interaction $F_{(1,16)} = 4.047$, $p = 0.0614$, genotype: $F_{(1,16)} = 59.15$, $p < 0.0001$, fraction $F_{(1,16)} = 332.4$, $p < 0.0001$ (P14 AnkB); $N = 5$, interaction $F_{(1,16)} = 0.7049$, $p = 0.4135$, genotype: $F_{(1,16)} = 68.89$, $p < 0.0001$, fraction $F_{(1,16)} = 85.56$, $p < 0.0001$ (P30 AnkB); $N = 5$, interaction $F_{(1,16)} = 0.0269$, $p = 0.8716$, genotype: $F_{(1,16)} = 3.025$, $p = 0.1012$, fraction $F_{(1,16)} = 143.3$, $p < 0.0001$ (P14 Cav2.1); $N = 5$, interaction $F_{(1,16)} = 10.47$, $p = 0.0052$, genotype: $F_{(1,16)} = 0.6942$, $p = 0.4170$, fraction $F_{(1,16)} = 181.7$, $p < 0.0001$ (P30 Cav2.1); $N = 5$, interaction $F_{(1,16)} = 0.4101$, $p = 0.5310$, genotype: $F_{(1,16)} = 0.1144$, $p = 0.7396$, fraction $F_{(1,16)} = 29.99$, $p < 0.0001$ (P14 syntaxin 1A); $N = 5$, interaction $F_{(1,16)} = 3.163$, $p = 0.0943$, genotype: $F_{(1,16)} = 6.345$, $p = 0.0228$, fraction $F_{(1,16)} = 34.34$, $p < 0.0001$ (P30 syntaxin 1A); $N = 4$, interaction $F_{(1,12)} = 2.869$, $p = 0.1161$, genotype: $F_{(1,12)} = 0.013$, $p = 0.9108$, fraction $F_{(1,12)} = 514.9$, $p < 0.0001$ (P14 PSD95); $N = 4$, interaction $F_{(1,12)} = 11.33$, $p = 0.0056$, genotype: $F_{(1,12)} = 0.2076$, $p = 0.6568$, fraction $F_{(1,12)} = 117.8$, $p < 0.0001$ (P30 PSD95)

2.5 Discussion

Our results presented here build on our knowledge of the relationship between the scaffold protein AnkB and the neuronal and pancreatic Cav2.1 protein, with important implications for understanding the mechanisms of extra-cardiac disease resulting from AnkB variants. Together our results suggest that AnkB regulates an intracellular pool of Cav2.1, a pool that may play an important role in neuronal homeostasis. Notably our findings suggest that this role is modulated by expression of AnkB variants associated with disease. Therefore dysregulation of Cav2.1 may present a possible mechanism for the pathogenicity of AnkB variants in the context of nervous system symptoms, such as seizure for AnkB p.S646F.

Taken together, our cellular expression system and cortical tissue experiments point to a new role for AnkB in the regulation of intracellular Cav2.1 levels. We found that overall Cav2.1 expression levels were higher in HEK293T cells transiently expressing AnkB than in control cells. Similarly, partial loss of AnkB in mouse cortex led to an overall decrease in Cav2.1 expression levels with no change in the synaptosome fraction. Although during development, Emx1-Cre turns on in the precursors of glutamatergic as well as glial cells (where AnkB is also expressed; refer to the transcriptome database for cerebral cortex cell by Zhang and colleagues (Zhang et al. 2014)), both Cav2.1 and syntaxin 1A are expressed markedly higher in neurons than glial cells. While we cannot rule out an indirect contribution of partial AnkB deletion in astrocytes on Cav2.1 expression levels in neurons, it is reasonable to speculate that the reduction in Cav2.1 levels in glutamatergic neurons is cell-autonomous. Furthermore, the changes in Cav2.1 expression levels occurred specifically in the intracellular

compartment but not at the cell surface or synaptosome fraction, suggesting that AnkB regulates the expression of an intracellular pool of Cav2.1. Regulation of Cav2.1 trafficking is likely critical for the development and maintenance of proper neuronal and pancreatic function. In neurons, Cav2.1 is localized not only to nerve terminals for neurotransmitter release, but also in dendrites and the cell body (Sakurai et al. 1996; Fu et al. 2017; Timmermann et al. 2002). Previous work on related VGCCs in different systems points to the possibility that intracellular Cav2.1 may serve as a reserve source, which under certain conditions or stimuli could be transported to the plasma membrane. For example, in bag cell neurons in Aplysia, Cav2 have been detected in intracellular punctae trafficking to distal lammellipodium upon PKC activation (Zhang et al. 2008). Similarly, a pool of N-type calcium channels, another presynaptic VGCC containing a synprint site (Sheng et al. 1994), can be found on secretory granules of IMR32 neuroblastoma cells that are translocated to the plasma membrane upon stimulation (Passafaro et al. 1996). Intracellular Cav2.1 could additionally or alternatively play a direct role in endomembrane compartment regulation. For example, a recent report revealed lysosomal localization of Cav2.1 in cultured cerebellar neurons, where it is required for lyso-endosome fusion/autophagosomal maturation (Tian et al. 2015). The authors of the study proposed that lysosomal Cav2.1 enables calcium efflux triggering SNARE mediated fusion of the lysosome to the endosome. Notably, in the present study, we found that the SNARE protein syntaxin 1A co-precipitates with AnkB, suggesting that it interacts either directly or indirectly through Cav2.1. We also found that partial loss of AnkB had a similar effect on syntaxin 1A expression levels as it did on Cav2.1 levels. Although it is possible that AnkB complexes with syntaxin 1A separately from

Cav2.1, considering the closely linked functions of Cav2.1 and syntaxin 1A, it is reasonable to speculate that AnkB, syntaxin 1A, and Cav2.1 form a complex. As AnkB is a well-known scaffolding protein, it may also serve here to stabilize Cav2.1 to the SNARE machinery. The interactions between AnkB, Cav2.1, and syntaxin 1A could serve to regulate intracellular Cav2.1 localization and function, and the regulation of the intracellular pool of Cav2.1 may be an important component of neuronal homeostasis.

Our work here also explored the effects of three different AnkB variants, p.S646F, p.Q879R, and p.E1458G, on AnkB itself as well as Cav2.1. AnkB p.S646F is associated with a presentation of seizures in carriers (Swayne et al. 2017). Alongside p. S646F, we also chose the human variant AnkB p.Q879R for its unique mutation site in the linker region required for AnkB localization (Anon n.d.; He et al. 2013). Lastly, we chose a variant occurring near the C-terminal regulatory domain, AnkB p.E1458G, well-known to cause cardiac abnormalities via interference with binding to ion channels in cardiomyocytes (Mohler et al. 2003; Mohler et al. 2005). We selected these variants to compare their effects on the trafficking of AnkB and Cav2.1. Our results suggest that expression of the AnkB variants caused somewhat different changes in Cav2.1 expression levels and activity, as well as AnkB trafficking (Fig 7). In terms of Cav2.1 localization, AnkB p.Q879R was the only variant that increased Cav2.1 surface levels, but this was only the case in the presence of $\alpha_2\delta_1$ and β_4. It is possible that Cav2.1 requires the assistance of these accessory subunits to exit the ER before the AnkB p.Q879R variant is able to localize Cav2.1 to the surface. Particularly, the β subunit influences VGCC trafficking, potentially by shifting the balance of ER retention and export signals, and prevents VGCC ubiquitination and degradation (Bichet et al. 2000; Fang & Colecraft

2011; Altier et al. 2011). Perhaps, without suppression of ER retention, Cav2.1 is unable to leave the ER, preventing AnkB from trafficking Cav2.1 to its proper subcellular location. With respect to Cav2.1 channel activity, although wildtype AnkB, AnkB p.S646F, and AnkB p.E1458G did not increase surface Cav2.1, all of the AnkB constructs increased Cav2.1-based VGCC peak current density. Since AnkB, AnkB p.S646F, and AnkB p.E1458G did not increase surface expression, it is reasonable to speculate that the increase current density associated with AnkB or AnkB variant expression are due to as yet undetermined effects on channel properties, although the precise mechanism is beyond the scope of the current study. Wildtype AnkB associated with surface proteins on its own while AnkB p.S646F and p.Q879R required the presence of Cav accessory subunits. AnkB p.E1458G did not significantly associate with surface proteins regardless of the presence of the accessory subunits. This suggests that mutations in AnkB can affect the trafficking of AnkB itself to the periphery, and that other neuronal proteins may play a role in assisting AnkB localization. In summary, the AnkB variants each resulted in a different combination of changes in Cav2.1 expression/localization, peak current density and AnkB localization.

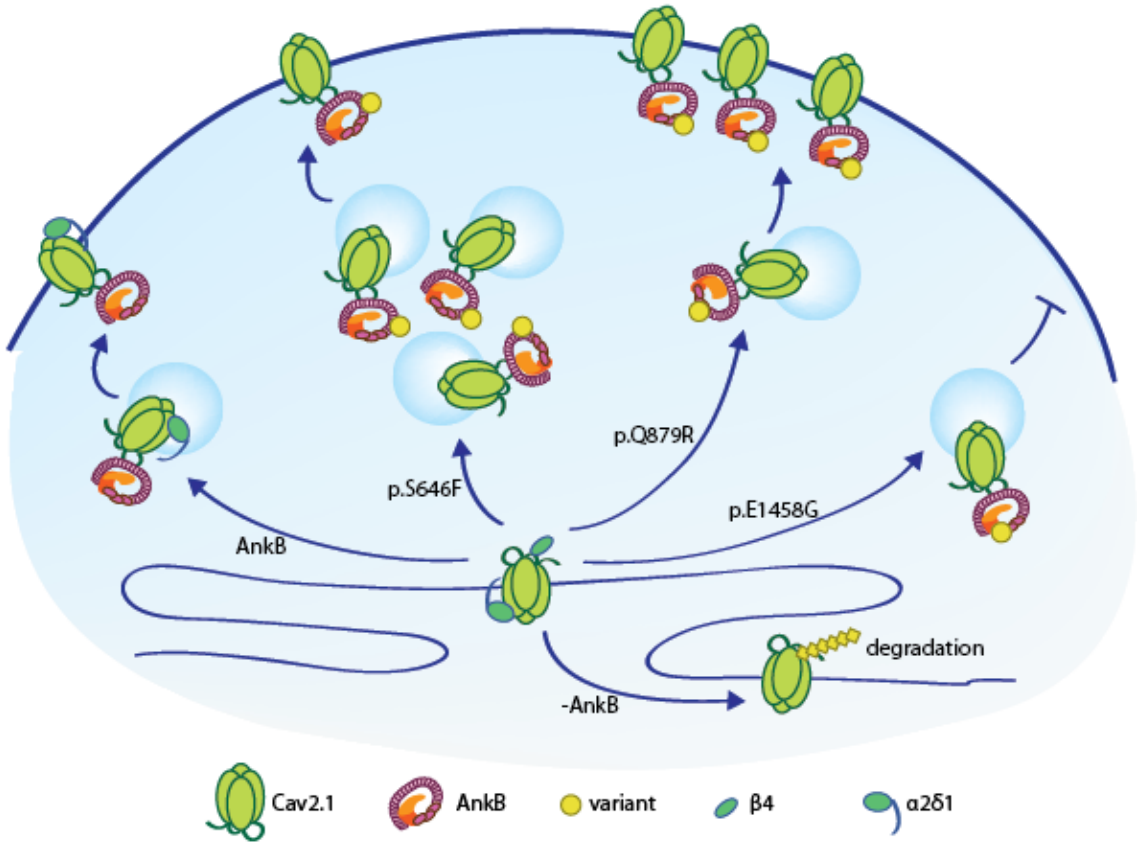

Figure 2.7 Working model of AnkB's regulation of Cav2.1.

In the absence of AnkB, Cav2.1 is expressed at a low level in the cell. In the presence of wildtype AnkB, Cav2.1 may be protected from degradation and therefore has higher intracellular levels while maintaining a low Cav2.1 surface level. With AnkB p.S646F variant, Cav2.1 is expressed at even higher level intracellularly but maintains the same low level on the surface. AnkB p.Q879R variant increases surface Cav2.1, while AnkB p.E1458G decreases surface Cav2.1. AnkB wildtype, p.S646F, and p.Q879R all had a surface associated pool in the presence of Cav accessory subunits. There was no significant surface associated pool with AnkB p.E1458G.

Together our findings provide evidence that AnkB regulates an intracellular pool of Cav2.1. This discovery sheds new light on the complex regulation of Cav2.1 necessary for proper neuronal function and will be important for understanding nervous system manifestations associated with AnkB variants.

3. General Discussion

Here I discovered a new role of AnkB, as a regulator of intracellular Cav2.1. Cav2.1 is a key ion channel in neurons, such that loss of function or mutations of Cav2.1 can lead to multiple neurological disorders (Damaj et al. 2015; Jouvenceau et al. 2001). I showed that AnkB variants lead to changes in Cav2.1 expression and localization, potentially pointing to the mechanism of AnkB pathogenicity. Particularly, this intracellular Cav2.1 may function as a stockpile of reserve Cav2.1 or may function in lysosomal fusion. Although AnkB did not alter synaptic Cav2.1, compensation by other ankyrins may dampen the effect of partial AnkB knockouts. Lastly, AnkB's effect on PSD95 suggests a role for AnkB at the postsynapse.

3.1 Crosstalk between Cav accessory subunits and the AnkB-Cav2.1 interaction

My results suggest potential crosstalk between AnkB, Cav2.1, Cavβ_4, and Cav$\alpha_2\delta_1$. Presence of Cavβ_4 and Cav$\alpha_2\delta_1$ led to surface association of AnkB variants p.S646F and p.Q879R. Only AnkB p.Q879R in the presence of Cavβ_4 and Cav$\alpha_2\delta_1$ led to increase Cav2.1 surface localization. Additionally, only wildtype AnkB led to increase surface localization of Cav$\alpha_2\delta_1$. These results suggest mutual regulation of the players at different points in Cav2.1 trafficking and function. The surface localization of Cav2.1 by AnkB p.Q879R only in the presence of accessory subunits suggests that AnkB trafficking of Cav2.1 requires assistance. Since Cavβ is involved in Cav2.1 ER export, possibly, AnkB trafficks Cav2.1 after it has exited the ER and is involved in either secretion or recycling of Cav2.1. Additionally, AnkB may be involved in Cav$\alpha_2\delta_1$ trafficking as only wildtype AnkB led to increase in Cav$\alpha_2\delta_1$ surface expression. Perhaps, AnkB variants are

defective in their regulation of Cav$\alpha_2\delta_1$ subunit. Interestingly, presence of Cav$\alpha_2\delta_1$ and Cavβ_4 led to surface association of AnkB p.S646F but did not change Cav2.1 surface expression. How Cav$\alpha_2\delta_1$ and Cavβ_4 are able to influence the localization of AnkB is unknown. Also, while AnkB p.S646F did not increase Cav2.1 surface levels, it increases Cav2.1 peak current density. This may be caused by changes in channel activity as oppose to changes in surface expression. The crosstalk between AnkB, Cav2.1, Cavβ_4, and Cav$\alpha_2\delta_1$ may ultimately lead to alteration in Cav2.1 and neuronal function, which is disrupted by AnkB variants.

Cav2.1 regulation could be the key to understanding seizures in AnkB p.S646F carriers. Carriers of Cav2.1 loss of function mutations exhibited seizures (Damaj et al. 2015). Additionally, two Cav2.1 mutation mouse models, the *leaner* mouse and *tottering* mouse, both show absence seizures (Fletcher et al. 1996). Particularly, the *tottering* mouse show great similarities to human absence epilepsy. As well, the *lethargic* mouse, with Cavβ_4 mutation and *ducky* mouse with Cav$\alpha_2\delta_2$ mutation also displayed seizure symptoms (Burgess et al. 1997; Barclay et al. 2001). The Cav subunits, Cavα_1, Cavβ, and Cav$\alpha_2\delta$, all seem to play a key role in neuronal function, that when mutated, can lead to abnormal neuronal discharges, seizures, and epilepsy phenotype. AnkB may play a part in regulating these crucial proteins necessary for normal neuronal firing. AnkB variants can alter surface levels of Cav2.1 and Cav$\alpha_2\delta_1$, while Cav accessory subunits can alter AnkB surface association. This crosstalk between Cav accessory subunits and the AnkB-Cav2.1 interaction may be the underlying mechanism behind AnkB p.S646F seizure symptoms and AnkB's association with epilepsy. Future work can look at the subcellular

localization and activity of Cav2.1 in various combinations of Cav2.1, AnkB, Cavβ, and Cav$\alpha_2\delta$ to dissect the crosstalk between these proteins.

3.2 Role of an intracellular pool of Cav2.1

In HEK293T cells, AnkB increased Cav2.1 expression levels without impacting Cav2.1 surface levels. Similarly, partial loss of AnkB in mouse cortices led to decrease Cav2.1 levels without affecting synaptosomal levels. This suggests that AnkB regulates Cav2.1 specifically in the intracellular compartment as oppose to the cell surface or synaptosome fractions. Although Cav2.1 is best known for its role in neurotransmitter release at the axon bouton, Cav2.1 is also localized to the somatodendritic compartment (He et al. 2018; Fu et al. 2017). Interestingly, an intracellular pool of Cav2 was discovered in bag cell neurons (Zhang et al. 2008). This intracellular Cav2 pool is recruited to the cell surface upon PKC activation. Likewise, an intracellular Cav2.2 pool was found in secretory granules that is also recruited to the cell surface upon stimulation (Passafaro et al. 1996). AnkB may regulate an intracellular pool of Cav2.1 that serves the same function of providing readily available Cav2.1 for recruitment to the cell surface when needed without waiting for *de novo* protein translation. Changes in levels of this intracellular pool can potentially alter the ability of neurons to respond to stimulation. Moreover, we found that syntaxin 1A were similarly affected by partial loss of AnkB. Like Cav2.1, syntaxin 1A is best known for its role at the presynapse in neurotransmitter release, where it mediates vesicles fusion and neurotransmitter release at specialized presynaptic active zones. In a recent study, syntaxin 1A was found in extra-synaptic compartment and was recruited to the synapse upon stimulation (Maidorn et al. 2019). Combined with my results that AnkB interacts with both Cav2.1 and syntaxin1A, a

preformed complex of AnkB-Cav2.1-syntaxin 1A may exist in an extra-synaptic compartment, ready for recruitment upon stimulation by PKC activation or depolarization. This preformed complex could act as a fast response to an immediate need for surface Cav2.1 capable of mediating neurotransmitter vesicle fusion. The number of calcium channels at the presynaptic active zones can have a large effect on neuronal responses. One method of strengthening a synapse is by increasing the number of calcium channels at the active zones, which increases the release probability of readily releasable vesicles (Sheng et al. 2012). The number of calcium channels can also affect short term plasticity, whereby a synapse with low number of calcium channels responded to repeated stimulation with facilitation whereas a high number of calcium channels responded with depression. Regulating intracellular Cav2.1 levels can provide the stockpile to make adjustments in synaptic strength at specific synapses. Modulating these neuronal responses could be an important component of plasticity

3.3 Other intracellular roles of Cav2.1: at the lysosome

Another potential role for an intracellular Cav2.1 is lysosomal fusion (Tian et al. 2015). Lysosomes are a necessary part of the autophagy pathway. Lysosomes contain the necessary environment and complement of enzymes to degrade unwanted materials such as misfolded protein (Ferguson 2019). Unwanted material are encapsulated into autophagosomes or endosomes and then fused with lysosomes. (Menzies et al. 2017). Defective lysosomal fusions can lead to diseases such as lysosomal storage disorders. Cav2.1 mutant neurons have lysosomal fusion defects and accumulate autophagic vacuoles (Tian et al. 2015). Specifically, calcium channel activity from intracellular rather than surface Cav2.1 is necessary for endo-lysosomal fusion. By increasing

intracellular Cav2.1, AnkB may affect rate of lysosomal fusion, disrupting neuronal homeostasis. Syntaxin 7 is the SNARE believed to be involved in lysosome-endosome fusion (Collins et al. 2002). Although syntaxin 1A is not known to be involved in lysosomal fusion, it remains a possibility. Like at the presynapse, Cav2.1 may trigger membrane-membrane fusion with syntaxin 1A and partner SNAREs via local increase in calcium concentration. Conversely, although my results indicate that AnkB interacts with both Cav2.1 and syntaxin 1A, it does not necessarily equate to an AnkB-Cav2.1-syntaxin 1A complex. With our co-immunoprecipitation set up, I cannot rule out the possibility that AnkB interacts with Cav2.1 and syntaxin 1A in two different complexes and have separate intracellular function.

My results point towards an intracellular pool of Cav2.1 regulated by AnkB. However, it is unknown in which subcellular compartment the pool resides. Determining where the AnkB-Cav2.1 complex exists within the neuron will shed light on the role of intracellular Cav2.1. Whether AnkB-Cav2.1 exists in secretory vesicles, lysosomes, or some other compartment will be important for unravelling this function.

3.4 Potential for compensation by other ankyrins

Partial loss of AnkB did not change Cav2.1 levels in synaptosomal fraction. It is possible that AnkB does not play a role in synaptic Cav2.1 trafficking. Another possibility is that since Cav2.1 plays such a crucial role in neurotransmitter release at the presynapse, other ankyrins or adaptors may compensate for the loss of AnkB and maintain a consistent level of Cav2.1 at the synapse. AnkR and AnkB have been shown to compensate for AnkG scaffolding when AnkG is lost. AnkG bridges Na^+ channels to the spectrin network at the AIS and nodes of Ranvier (Ho et al. 2014). Loss of AnkG

specifically in peripheral sensory neurons or retinal ganglion cells leads to loss of Na^+ channel clustering at the AIS. However, at the nodes of Ranvier, AnkR compensates for AnkG loss and co-localizes with Na^+ channels at the nodes of Ranvier. Interestingly, loss of AnkG specifically in myelinating glia was compensated by AnkB (Chang et al. 2014). Potentially, a similar compensation could be at work here in the localization of Cav2.1 to the synapse. In order to maintain an essential minimal level of Cav2.1 at the synapse, either AnkG or AnkR may localize synaptic Cav2.1.

3.5 Role of AnkB at the postsynaptic compartment

Partial loss of AnkB does not affect Cav2.1 or syntaxin 1A in synaptosomal fraction, but it increases PSD95 in synaptosomal fraction at P30. AnkB interacts with a variety of proteins and likely regulates different proteins in a different manner. For Cav2.1, AnkB is involved with intracellular expression. For PSD95, AnkB may be involved with synaptic expression. A recent preprint study investigated the role of giant 440 kDa AnkB (Yang et al. 2018). AnkB was mutated so that giant AnkB was truncated without affecting canonical 220 kDa AnkB. In these mice, pyramidal neurons from P28 cortex exhibited an increased number of spines. These mutant mice also displayed abnormal social responses. In my results, partial loss of AnkB increased PSD95 in the synaptosomal fraction. As PSD95 is a postsynaptic marker, it is likely that AnkB increases the number of PSD95 at postsynapses or increases the number of spines that contains PSD95. ASD is associated with increased number of spines (Penzes et al. 2011). The association of AnkB to ASD may be due to an increased in the number of postsynaptic structures caused by mutations in AnkB.

3.6 Thesis summary

The results here provide new insights into the working of AnkB. The discovery that AnkB regulates an intracellular pool of Cav2.1 suggests exciting new roles for AnkB and Cav2.1 in neuronal function and potential mechanism for the pathogenicity observed in AnkB variants. Uncovering AnkB's role in diverse settings will be an exciting frontier for future works.

Bibliography

Abdi, K.M. et al., 2006. Isoform specificity of ankyrin-B: A site in the divergent C-terminal domain is required for intramolecular association. *Journal of Biological Chemistry*, 281(9), pp.5741–5749.

Altier, C. et al., 2011. The Cavβ subunit prevents RFP2-mediated ubiquitination and proteasomal degradation of L-type channels. *Nature Neuroscience*, 14(2), pp.173–182.

Barclay, J. et al., 2001. Ducky mouse phenotype of epilepsy and ataxia is associated with mutations in the Cacna2d2 gene and decreased calcium channel current in cerebellar Purkinje cells. *The Journal of neuroscience*, 21(16), pp.6095–104.

Bennett, V., 1979. Immunoreactive forms of human erythrocyte ankyrin are present in diverse cells and tissues. *Nature*, 281, pp.597–599.

Bennett, V. & Healy, J., 2009. Membrane domains based on ankyrin and spectrin associated with cell-cell interactions. *Cold Spring Harbor perspectives in biology*, 1(6).

Bennett, V. & Lorenzo, D.N., 2013. *Spectrin- and Ankyrin-Based Membrane Domains and the Evolution of Vertebrates* 1st ed., Elsevier Inc.

Bennett, V. & Stenbuck, P.J., 1980. Association between Ankyrin and the Cytoplasmic Domain of Band 3 Isolated from the Human Erythrocyte Membrane. *The Journal of Biological Chemistry*, 255(13), pp.6424–6432.

Bernstein, G.M. & Jones, O.T., 2007. Kinetics of internalization and degradation of N-type voltage-gated calcium channels: Role of the α2/δ subunit. *Cell Calcium*, 41(1), pp.27–40.

Bichet, D. et al., 2000. The I-II loop of the Ca2+ channel alpha1 subunit contains an endoplasmic reticulum retention signal antagonized by the beta subunit. *Neuron*, 25(1), pp.177–190.

Buraei, Z. & Yang, J., 2010. The β Subunit of Voltage-Gated Ca 2+ Channels . *Physiological Reviews*, 90(4), pp.1461–1506.

Burgess, D.L. et al., 1997. Mutation of the Ca2+ channel β subunit gene Cchb4 is associated with ataxia and seizures in the lethargic (lh) mouse. *Cell*, 88(3), pp.385–392.

Cassidy, J.S. et al., 2014. Functional exofacially tagged N-type calcium channels elucidate the interaction with auxiliary 2 -1 subunits. *Proceedings of the National Academy of Sciences*, 111(24), pp.8979–8984.

Catterall, W.A., 2011. Voltage-Gated Calcium Channels. *Cold Spring Harb Perspect Biol*, 3, p.a003947.

Catterall, W.A., Leal, K. & Nanou, E., 2013. Calcium channels and short-term synaptic plasticity. *Journal of Biological Chemistry*, 288(15), pp.10742–10749.

Chang, K.-J. et al., 2014. Glial ankyrins facilitate paranodal axoglial junction assembly. *Nature Neuroscience*, 17(12), pp.1673–1681.

Collins, M.O. et al., 2006. Molecular characterization and comparison of the components and multiprotein complexes in the postsynaptic proteome. *Journal of*

Neurochemistry, 97, pp.16–23.

Collins, R.F. et al., 2002. Syntaxins 13 and 7 Function at Distinct Steps During Phagocytosis. *The Journal of Immunology*, 169(6), pp.3250–3256.

Cornet, V. et al., 2002. Multiple determinants in voltage-dependent P/Q calcium channels control their retention in the endoplasmic reticulum. *European Journal of Neuroscience*, 16(5), pp.883–895.

Cunha, S.R., Bhasin, N. & Mohler, P.J., 2007. Targeting and stability of Na/Ca exchanger 1 in cardiomyocytes requires direct interaction with the membrane adaptor ankyrin-B. *Journal of Biological Chemistry*, 282(7), pp.4875–4883.

Cunha, S.R. & Mohler, P.J., 2009. Ankyrin protein networks in membrane formation and stabilization. *J. Cell. Mol. Med.*, 13(11), pp.4364–4376.

Damaj, L. et al., 2015. CACNA1A haploinsufficiency causes cognitive impairment , autism and epileptic encephalopathy with mild cerebellar symptoms. *European Journal of Human Genetics*, 23, pp.1505–1512.

Davies, A. et al., 2010. The 2 subunits of voltage-gated calcium channels form GPI-anchored proteins, a posttranslational modification essential for function. *Proceedings of the National Academy of Sciences*, 107(4), pp.1654–1659.

Devereaux, K. et al., 2013. Regulation of Mammalian Autophagy by Class II and III PI 3-Kinases through PI3P Synthesis. *PLoS ONE*, 8(10), pp.10–12.

Dolphin, A.C., 2018. Voltage-gated calcium channel α2δ subunits: an assessment of proposed novel roles. *F1000Research*, 7(0), p.1830.

El-Husseini, A..-D. et al., 2000. PSD-95 involvement in maturation of excitatory synapses. *Science*, 290, pp.1364–1368.

Exome variant server HLBI, 2019. Exome Variant Server HLBI GO exome Sequencing Project (ESP), Seattle, WA (URL: http://evs.gs.washington.edu/EVS/) Accessed May 22, 2019

Fang, K. & Colecraft, H.M., 2011. Mechanism of auxiliary β-subunit-mediated membrane targeting of L-type (CaV1.2) channels. *Journal of Physiology*, 589(18), pp.4437–4455.

Ferguson, S.M., 2019. Neuronal lysosomes. *Neuroscience Letters*, 697(April), pp.1–9.

Fletcher, C.F. et al., 1996. Absence epilepsy in tottering mutant mice is associated with calcium channel defects. *Cell*, 87(4), pp.607–617.

Fu, S.-J. et al., 2017. Ubiquitin Ligase RNF138 Promotes Episodic Ataxia Type 2-Associated Aberrant Degradation of Human Ca_v 2.1 (P/Q-Type) Calcium Channels. *The Journal of Neuroscience*, 37(9), pp.2485–2503.

Galiano, M.R. et al., 2012. A distal axonal cytoskeleton forms an intra-axonal boundary that controls axon initial segment assembly. *Cell*, 149(5), pp.1125–1139.

Garcia-Caballero, A. et al., 2018. T-type calcium channels functionally interact with spectrin (α/β) and ankyrin B. *Molecular Brain*, 11, p.24.

Gil, O.D. et al., 2003. Ankyrin binding mediates L1CAM interactions with static components of the cytoskeleton and inhibits retrograde movement of L1CAM on the cell surface. *The Journal of Cell Biology*, 162(4), pp.719–730.

Gorski, J.A. et al., 2002. Cortical excitatory neurons and glia, but not GABAergic

neurons, are produced in the Emx1-expressing lineage. *The Journal of Neuroscience*, 22(15), pp.6309–6314.

Guo, W. et al., 2017. Identifying and Analyzing Novel Epilepsy-Related Genes Using Random Walk with Restart Algorithm. *BioMed Research International*, 2017, pp.1–13.

He, M., Tseng, W.C. & Bennett, V., 2013. A single divergent exon inhibits ankyrin-B association with the plasma membrane. *Journal of Biological Chemistry*, 288(21), pp.14769–14779.

He, R. et al., 2018. New Insights Into Interactions of Presynaptic Calcium Channel Subtypes and SNARE Proteins in Neurotransmitter Release. *Frontiers in Molecular Neuroscience*, 11(July), pp.1–11.

Heyne, H.O. et al., 2018. De novo Variants in Neurodevelopmental Disorders with Epilepsy. *Nature Genetics*, 50, pp.1048–1053.

Hirano, M. et al., 2017. C-terminal splice variants of P/Q-type Ca2+ channel Cav2.1 α1 subunits are differentially regulated by Rab3-interacting molecular proteins. *J. BIol. Chem*, 292, pp.9365–9381.

Ho, T.S.-Y. et al., 2014. A Hierarchy of Ankyrin/Spectrin Complexes Clusters Sodium Channels at N odes of Ranvier. *Nat. Neurosci*, 17(12), pp.1664–1672.

Imbrici, P. et al., 2004. Dysfunction of the brain calcium channel Cav2.1 in absence epilepsy and episodic ataxia. *Brain*, 127, pp.2682–2692.

Indriati, D.W. et al., 2013. Quantitative localization of Cav2.1 (P/Q-Type) voltage dependent calcium channels in Purkinje cells: Somatodendritic gradient and distinct somatic coclustering with calcium-activated potassium channels. *J. Neurosci*, 33(8), pp.3668–3678.

Iossifov, I. et al., 2014. The contribution of de novo coding mutations to autism spectrum disorder. *Nature*, 515(7526), pp.216–221.

Islam, Z. et al., 2018. International Journal of Biological Macromolecules New paradigm in ankyrin repeats : Beyond protein-protein interaction module. *International Journal of Biological Macromolecules*, 109, pp.1164–1173.

Jay, S.D. et al., 1991. Structural characterization of the dihydropyridine-sensitive calcium channel α2-subunit and the associated δ peptides. *Journal of Biological Chemistry*, 266, pp.3287–3293.

Jordan, B.A. et al., 2004. Identification and Verification of Novel Rodent Postsynaptic Density Proteins. *Molecular & Cellular Proteomics*, pp.857–871.

Jouvenceau, A. et al., 2001. Human epilepsy associated with dysfunction of the brain P/Q-type calcium channel. *Lancet*, 358(9284), pp.801–807.

Jun, K. et al., 1999. Ablation of P/Q-type Ca2+ channel currents , altered synaptic transmission, and progressive ataxia in mice lacking the α1A -subunit. *PNAS*, 96(26), pp.15245–15250.

Kaeser, P.S. et al., 2011. RIM proteins tether Ca2+ channels to presynaptic active zones via a direct PDZ-domain interaction. *Cell*, 144(2), pp.282–295.

Kang, M.-G. et al., 2006. A functional AMPA receptor-calcium channel complex in the postsynaptic membrane. *Proceedings of the National Academy of Sciences of the*

United States of America, 103(14), pp.5561–5566.

Kline, C.F. et al., 2014. Ankyrin-B regulates Cav2.1 and Cav2.2 channel expression and targeting. *Journal of Biological Chemistry*, 289(8), pp.5285–5295.

Koenig, S.N. & Mohler, P.J., 2017. The evolving role of ankyrin-B in cardiovascular disease. *Heart Rhythm*, 14(12), pp.1884–1889.

Lencesova, L. et al., 2004. Plasma Membrane-Cytoskeleton-Endoplasmic Reticulum Complexes in Neurons and Astrocytes. *Journal of Biological Chemistry*, 279(4), pp.2885–2893.

Liu, J.J., 2017. Regulation of dynein-dynactin-driven vesicular transport. *Traffic*, 18(6), pp.336–347.

Lorenzo, D.N. et al., 2014. A PIK3C3-Ankyrin-B-Dynactin pathway promotes axonal growth and multiorganelle transport. *Journal of Cell Biology*, 207(6), pp.735–752.

Lorenzo, D.N. et al., 2015. Ankyrin-B metabolic syndrome combines age-dependent adiposity with pancreatic β cell insufficiency. *Journal of Clinical Investigation*, 125(8), pp.3087–3102.

Lorenzo, D.N. & Bennett, V., 2017. Cell-autonomous adiposity through increased cell surface GLUT4 due to ankyrin-B deficiency. *PNAS*, 114, pp.12743–12748.

Maidorn, M. et al., 2019. Nanobodies reveal an extra-synaptic population of SNAP-25 and Syntaxin 1A in hippocampal neurons. *mAbs*, 11(2), pp.305–321.

Maltez, J.M. et al., 2005. Essential Cavβ modulatory properties are AID-independent. *Nature Structural and Molecular Biology*, 12(4), pp.372–377.

Menzies, F.M. et al., 2017. Autophagy and Neurodegeneration: Pathogenic Mechanisms and Therapeutic Opportunities. *Neuron*, 93(5), pp.1015–1034.

Michaely, P. et al., 2002. Crystal structure of a 12 ANK repeat stack from human ankyrinR. *The EMBO Journal*, 21(23), pp.6387–6396.

Mochida, S., 2000. Protein-protein interactions in neurotransmitter release. *Neuroscience Research*, 36(3), pp.175–182.

Mohler, P.J. et al., 2004. A cardiac arrhythmia syndrome caused by loss of ankyrin-B function. *Proceedings of the National Academy of Sciences of the United States of America*, 101(24), pp.9137–42.

Mohler, P.J. et al., 2003. Ankyrin-B mutations causes type 4 long-QT cardiac arrhythmia and sudden cardiac death. *Nature*, 421, pp.634–639.

Mohler, P.J. et al., 2007. Ankyrin-B syndrome: enhanced cardiac function balanced by risk of cardiac death and premature senescence. *PloS one*, 2(10), p.e1051.

Mohler, P.J., Le Scouarnec, S., Denjoy, I., Lowe, J.S., Guicheney, P., Caron, L., Driskell, I.M., Schott, J.-J., et al., 2007. Defining the Cellular Phenotype of "Ankyrin-B Syndrome" Variants. *Circulation*, 115(4).

Mohler, P.J., Le Scouarnec, S., Denjoy, I., Lowe, J.S., Guicheney, P., Caron, L., Driskell, I.M., Schott, J.J., et al., 2007. Defining the cellular phenotype of "ankyrin-B syndrome" variants: Human ANK2 variants associated with clinical phenotypes display a spectrum of activities in cardiomyocytes. *Circulation*, 115(4), pp.432–441.

Mohler, P.J., Davis, J.Q. & Bennett, V., 2005. Ankyrin-B coordinates the Na/K ATPase, Na/Ca exchanger, and InsP3 receptor in a cardiac T-tubule/SR microdomain. *PLoS*

Biology, 3(12), pp.2158–2167.

Mohler, P.J., Gramolini, A.O. & Bennett, V., 2002. The ankyrin-B C-terminal domain determines activity of ankyrin-B/G chimeras in rescue of abnormal inositol 1,4,5-trisphosphate and ryanodine receptor distribution in ankyrin-B (-/-) neonatal cardiomyocytes. *Journal of Biological Chemistry*, 277(12), pp.10599–10607.

Nanou, E., Scheuer, T. & Catterall, W.A., 2016. Calcium sensor regulation of the Cav2.1 Ca2+ channel contributes to long-term potentiation and spatial learning. *Proceedings of the National Academy of Sciences*, 113(46), pp.13209–13214.

Ogawa, Y., 2006. Spectrins and AnkyrinB Constitute a Specialized Paranodal Cytoskeleton. *Journal of Neuroscience*, 26(19), pp.5230–5239.

Page, K.M., Rothwell, S.W. & Dolphin, A.C., 2016. The CaVβ subunit protects the I-II loop of the voltage-gated calcium channel CaV2.2 from proteasomal degradation but not oligoubiquitination. *Journal of Biological Chemistry*, 291(39), pp.20402–20416.

Passafaro, M. et al., 1996. N-type Ca 2+ channels are present in secretory granules and are transiently translocated to the plasma membrane during regulated exocytosis. *Journal of Biological Chemistry*, 271(47), pp.30096–30104.

Passafaro, M. et al., 1994. ω-conotoxin and Cd2+ stimulate the recruitment to the plasmamembrane of an intracellular pool of voltage-operated Ca2+ channels. *Neuron*, 12(2), pp.317–326.

Patel, R. & Dickenson, A.H., 2016. Mechanisms of the gabapentinoids and α2δ-1 calcium channel subunit in neuropathic pain. *Pharmacology Research and Perspectives*, 4(2), pp.1–13.

Peng, J. et al., 2004. Semiquantitative proteomic analysis of rat forebrain postsynaptic density fractions by mass spectrometry. *Journal of Biological Chemistry*, 279(20), pp.21003–21011.

Penzes, P. et al., 2011. Dendritic spine pathology in neuropsychiatric disorders. *Nat Neurosci*, 14(3), pp.285–293.

Pietrobon, D., 2010. Insights into migraine mechanisms and CaV2.1 calcium channel function from mouse models of familial hemiplegic migraine. *Journal of Physiology*, 588(11), pp.1871–1878.

Qu, F. et al., 2016. Ankyrin-B is a PI3P effector that promotes polarized α5β1-integrin recycling via recruiting RabGAP1L to early endosomes. *eLife*, 5, pp.1–25.

Rettig, J. et al., 1996. Isoform-specific interaction of the alpha1A subunits of brain Ca2+ channels with the presynaptic proteins syntaxin and SNAP-25. *Proceedings of the National Academy of Sciences of the United States of America*, 93(14), pp.7363–7368.

Rubeis, S. De et al., 2014. Synaptic, transcriptional, and chromatin genes disrupted in autism. *Nature*, 515(7526), pp.209–215.

Sakurai, T. et al., 1996. Biochemical-properties and subcellular-distribution of the bi and rba isoforms of alpha(1a) subunits of brain calcium channels. *Journal Of Cell Biology*, 134(2), pp.511–528.

Sanchez-arias, J.C. et al., 2019. Pannexin 1 regulates network ensembles and dendritic spine development in cortical neurons. *eNeuro*, 6(3), pp.1–19.

Schorge, S. & Rajakulendran, S., 2012. The P/Q channel in human disease: Untangling the genetics and physiology. *Wiley Interdisciplinary Reviews: Membrane Transport and Signaling*, 1(3), pp.311–320.

Scotland, P. et al., 1998. Nervous system defects of ankyrinB (-/-) mice suggest functional overlap between the cell adhesion molecule L1 and 440-kD ankyrinB in premyelinated axons. *The Journal of Cell Biology*, 143(5), pp.1305–1315.

Sheng, J. et al., 2012. Calcium-channel number critically influences synaptic strength and plasticity at the active zone. *Nature Neuroscience*, 15(7), pp.998–1006.

Sheng, Z.H. et al., 1994. Identification of a syntaxin-binding site on N-type calcium channels. *Neuron*, 13(6), pp.1303–1313.

Simms, B.A. & Zamponi, G.W., 2014. Neuronal voltage-gated calcium channels: Structure, function, and dysfunction. *Neuron*, 82(1), pp.24–45.

Smith, K.R. & Penzes, P., 2018. Ankyrins: Roles in synaptic biology and pathology. *Molecular and Cellular Neuroscience*, 91(May), pp.131–139.

Smith, S.A. et al., 2015. Dysfunction in the βII spectrin-dependent cytoskeleton underlies human arrhythmia. *Circulation*, 131(8), pp.695–708.

Snutch, T.P. et al., 1990. Rat brain expresses a heterogeneous family of calcium channels. *Proceedings of the National Academy of Sciences*, 87, pp.3391–3395.

Swayne, L.A. et al., 2017. Novel variant in the ANK2 membrane-binding domain is associated with Ankyrin-B syndrome and structural heart disease in a first nations population with a high rate of long QT syndrome. *Circulation: Cardiovascular Genetics*, 10, p.e001537.

Tétreault, M.P. et al., 2016. Identification of glycosylation sites essential for surface expression of the CaVα2δ1 subunit and modulation of the cardiac CaV1.2 channel activity. *Journal of Biological Chemistry*, 291(9), pp.4826–4843.

Tian, X. et al., 2015. A Voltage-Gated Calcium Channel Regulates Lysosomal Fusion with Endosomes and Autophagosomes and Is Required for Neuronal Homeostasis. *PLoS Biology*, 13(3), pp.1–25.

Timmermann, D.B. et al., 2002. Distribution of high-voltage-activated calcium channels in cultured γ-aminobutyric acidergic neurons from mouse cerebral cortex. *Journal of Neuroscience Research*, 67(1), pp.48–61.

Tsien, R.W. & Barrett, C.F., *A Brief History of Calcium Channel Discovery*,

Verpelli, C. et al., 2012. Scaffold proteins at the postsynaptic density. *Adv Exp Med Biol*, 970, pp.29–61.

Wang, C. et al., 2014. Structural basis of diverse membrane target recognitions by ankyrins. *eLife*, 3, pp.1–22.

Weiss, N. & Zamponi, G.W., 2017. Trafficking of neuronal calcium channels. *Neuronal Signaling*, 1(1), p.NS20160003.

Wiser, O., Bennett, M.K. & Atlas, D., 1996. Functional interaction of syntaxin and SNAP-25 with voltage-sensitive L- and N-type Ca2+ channels. *The EMBO journal*, 15(16), pp.4100–10.

Yamankurt, G. et al., 2012. Ankyrin-Based Trafficking and Scaffolding of Membrane Proteins: Implications for Plasma Membrane Stability, Formation, and

Specialization. *J Proteomics Bioinform S*, 4(10), p.2.

Yang, R. et al., 2018. A giant ankyrin-B mechanism for neuro-diversity/divergence through stochastic ectopic axon projections. *http://dx.doi.org/10.1101/479741*.

Zhang, Y. et al., 2014. An RNA-Sequencing transcriptome and splicing database of glia, neurons, and vascular cells of the cerebral cortex. *Journal of Neuroscience*, 34(36), pp.11929–11947.

Zhang, Y. et al., 2008. PKC-induced intracellular trafficking of Cav2 precedes its rapid recruitment to the plasma membrane. *Journal of Neuroscience*, 28(10), pp.2601–2612.